

SHOCK-WAVE PROCESSING OF  
POWDER MIXTURES

Thesis by  
Barry Robert Krueger

In Partial Fulfillment of the Requirements  
for the Degree of  
Doctor of Philosophy

Advisor: Prof. Thad Vreeland, Jr.

California Institute of Technology  
Pasadena California

1991

(Submitted May 6, 1991)

In Memory of Barry Robert Krueger

July 19, 1965 – October 29, 1990

Dedicated to his family Reinhold, Evelyn, Linda, and Rita Krueger  
and to Anita Harper

## ACKNOWLEDGEMENTS

The assistance of Barry's friend and office-mate, Andrew H. Mutz, in developing the facilities used in this research and in the compilation of this thesis is gratefully acknowledged. Zezhong Fu generously assisted in the running of the differential thermal analyses.

Barry was a promising scientist and a valued friend who made many positive contributions to the Caltech community. His colleagues and the many undergraduates who came to know him fondly remember the exuberant way he lived his life.

Thad Vreeland, Jr.

Professor of Materials Science

Caltech, April 1991

TABLE OF CONTENTS

Dedication ..... *ii*

Acknowledgements ..... *iii*

Abstract ..... *vi*

1. INTRODUCTION ..... 1

    REFERENCES..... 5

2. CALCULATION OF THE SHOCK HUGONIOT FOR MIXTURES ..... 6

    2.1 "A Hugoniot Theory for Solid and Powder Mixtures,"  
         by Barry R. Krueger and Thad Vreeland, Jr., published  
         in the Journal of Applied Physics, January 1991. .... 6

3. SHOCK INITIATION OF THE REACTION FORMING NiSi ..... 33

    3.1 "Shock Initiated Chemical Reactions in 1:1 Atomic Percent  
         Ni/Si Powder Mixtures," by B. Krueger and T. Vreeland, Jr.,  
         to appear in the Proceedings of the International Conference  
         on High-Strain-Rate Phenomena in Materials, UCSD  
         (Explomet '90, in Press). .... 33

    3.2 "Correlation of Shock Initiated and Thermally Initiated  
         Chemical Reactions in a 1:1 Atomic Ratio Nickel-Silicon  
         Mixture," by Barry R. Krueger, Andrew H. Mutz, and Thad  
         Vreeland, Jr., submitted to the Journal of Applied Physics,  
         March 1991. .... 44

4 . SHOCK INITIATION OF THE REACTION FORMING  $Ti_5Si_3$  ..... 68

    4.1 "Shock Induced Reactions in 5:3 Atomic Ratio  
         Titanium/Crystalline Silicon Powder Mixtures,"  
         by B. R. Krueger, A. H. Mutz and T. Vreeland, Jr.,  
         submitted to Metallurgical Transactions, A, March 1991. .... 68

5. SHOCK CONSOLIDATION OF A METALLIC GLASS ..... 79

5.1 "Shock Wave Consolidation of a Ni-Cr-Si B Metallic Glass," by J.  
Bach, B. R. Krueger and B. F. Fultz, Materials Lett.,  
(1991, in press) ..... 79

## ABSTRACT

The effects of shock waves on the initiation of exothermic chemical reactions in mixtures of powders is explored experimentally and compared to thermal initiation at atmospheric pressure in this thesis. A full understanding of shock-initiated chemical reactions and shock compaction of composites requires knowledge of the Hugoniot of the mixture. A model for calculation of the shock Hugoniot of non-reacting solid or powder mixtures up to moderate pressures using only thermodynamic properties of the components is presented. In addition, conditions for the production of dense, bulk samples of a metallic glass from the metastable powder are determined.

Previous models for the Hugoniot of a mixture assume the components in the shock front are in mutual thermal equilibrium, and use measured or calculated Hugoniot data for the components. The model proposed in this thesis does not presuppose either the relative magnitude of the thermal and elastic energies or temperature equilibrium between the components. It assumes the components are at equal pressures and have equal particle velocities. For a mixture, it is shown that the conservation equations define a Hugoniot surface, and that the ratio of the thermal energy of the components determines where on that surface the shocked state of the mixture lies. This ratio, which may strongly affect shock-initiated chemical reactions and the properties of consolidated mixtures, is found to have only a minor effect on the Hugoniot. It is also found that the Hugoniots of solids and solid mixtures are sensitive to the pressure derivative of the isentropic bulk moduli of the components at constant entropy.

The initiation of the reaction forming the compound NiSi from elemental powders by shock waves of varying energy and pressure and by thermal initiation at

atmospheric pressure was investigated. Using plane wave shock geometry with well-defined shock pressure and energy, it was determined that a sharp energy threshold, between 384 and 396 J/g, exists for the initiation of the reaction (with 20  $\mu\text{m}$  to 45  $\mu\text{m}$  Ni and -325 mesh Si). The threshold energy range heats the powder mixture to a temperature between 631 and 648° C (with no chemical reaction) after local thermal equilibration is achieved. The reaction goes to completion when the shock energy is above the threshold energy, and melting of the compound is indicated. Differential thermal analyses (DTA) of powder mixtures of Ni and Si (1:1 atomic ratio) at atmospheric pressure show the reaction starts at a temperature which depends upon the porosity of the mixture. Higher porosities give higher initiation temperatures. Reaction starts at about 900° C in a mixture with 50% porosity and at about 650° C in a sample statically pressed to 23% porosity. The sharp energy threshold for the initiation of the reaction, and the correlation with the shock temperature and the reaction initiation temperature in the DTA indicates that the homogeneous temperature determines whether or not the reaction occurs rather than local particle conditions of temperature or pressure as has been proposed in the literature.

The conditions for initiation and propagation of the reaction forming  $\text{Ti}_5\text{Si}_3$  from elemental powders (5:3 atomic ratio) of varying porosity have been investigated using shock waves of different pressure in vacuum, and using hot wire ignition in an argon atmosphere. In powders with a high initial porosity, evacuated to 0.1 torr, a low energy regime (producing low shock pressures) triggers the reaction in the presence of residual oxygen while no reaction is observed with a 128% higher shock energy and a lower initial porosity (producing a higher shock pressure) in an inert residual gas. Hot wire ignition of porous powder at room temperature initiates a self-propagating high temperature reaction (SHS) in air or

(less readily) in an Ar atmosphere, while the Ni/Si powder must be heated to allow the reaction to propagate in high or low porosity mixtures. These observations are compared to published work on self-sustaining reactions in multilayer films.

## 1. INTRODUCTION

The isentropic compressibility in most materials decreases with increasing pressure. Then the velocity of propagation of acoustical disturbances increases with pressure. A pressure wave whose profile is not constant will therefore steepen as higher pressure components overtake the low pressure components at the beginning of the wave. A narrow shock transition region is reached across which there is a jump in the pressure profile and the width of this region, the shock front, is on the order of the atomic spacing in solids, the mean-free-path in gasses, and the particle size in powders. The theory of the formation and propagation of shock waves is covered in several comprehensive texts.[1,2]

Shock-induced chemistry in solids was explored as early as 1920 in an attempt to synthesize diamond.[3] Explosive loading of graphite produced the first successful synthesis of diamond in the early 60's.[4] Early experiments on chemical reactions in solids initiated by shock wave loading were conducted in the 50's and 60's,[5] and continued in Russia in the 70's and 80's.[6,7] An assessment of work on chemical synthesis in metallic and inorganic substances under high pressure shock loading was given by R. A. Graham et al., in which examples of shock-enhanced solid state reactivity are given.[8] R. A. Graham has attributed the shock-enhancement to what he has termed "catastrophic shock" conditions as opposed to "benign" conditions of temperature and pressure increase associated with the shock.[9] The "catastrophic" shock conditions include: a) the breaking of chemical bonds, b) the formation of activated complexes, c) mass mixing, and d) introduction of crystal defects such as vacancies which accelerate processes such as atomic diffusion.

This thesis presents the results of research on shock wave processing of metallic materials under controlled plane-wave shock conditions. Changes in

particle velocity, internal energy, and pressure across a steady-state plane shock front are obtained from the equations of conservation of mass, momentum and energy (the Rankine-Hugoniot equations). The set of shock states that a medium can reach across a single shock wave, from a known initial state, is obtained from knowledge of the material properties in the form of pressure vs. specific volume, pressure vs. particle velocity, or shock velocity vs. particle velocity (Hugoniots of the medium). Hugoniots of a number of solids have been obtained experimentally.[10] Theoretical models have been developed for obtaining Hugoniots of solid mixtures from Hugoniots of their components by McQueen,[11] and by use of a thermodynamically consistent procedure, based on the Gibbs free energy by Duvall and Taylor.[12] Both of these models assume temperature equilibration of the mixture components occurs in the shock front. This assumption is not accurate, as recognized by Duval and Taylor, but it introduces little error in a solid as opposed to a powder mixture because in the shocked solid the elastic energy is larger than the thermal energy. The opposite is true in a shocked powder in which the pressure is sufficient to reduce the porosity significantly. Chapter 1 of this thesis presents a model from which the Hugoniot of solid or porous two-component mixtures can be calculated (up to moderate pressures) from thermodynamic properties of the components. The model treats non-reacting mixtures and does not presuppose either the relative magnitude of the thermal and elastic energies or temperature equilibrium between the two components.

Shock initiated chemical reactions may have strong effects on the Rankine-Hugoniot relationships and cause changes in the Hugoniot as well. These result from the additional source (or sink) of chemical energy, from volume changes between reactants and products, and from changes in thermodynamic properties. In order to account for these effects on the shock parameters, the rate of reaction as well as the property changes must be known. The rate of reaction is typically an

exponential function of temperature. Surface temperatures in shocked, non-reacting powders have been measured, and it is found that: a) the temperature rises during passage of the shock front in a time very nearly equal to the time for the shock wave to travel one particle diameter (i.e., the shock rise time which is a few tens of nanoseconds for typical powders of about 50  $\mu\text{m}$  diameter), b) the surface temperature of the particles reaches a maximum (limited by the melting point of the powder material) at the end of the shock rise time and then decreases as heat flows to cooler particle interiors, and c) the temperature reached after thermal equilibration of the particles (the homogeneous temperature) correlates well with heating by essentially all of the shock energy calculated from the Rankine-Hugoniot relations.[11] Surface melting plays an important role in helping to bond particles together, and the rapid cooling (rates up to  $10^{10}$  degrees C/s) are sufficient to retain properties which are metastable at the homogeneous temperature or to form metastable properties from the shock-formed melt.

Quantitative data on the rate of shock induced chemical reactions in solid materials is not available, but a large body of data has been obtained in a number of systems for thermally induced reactions at atmospheric pressure. "Explosive" reactions (which propagate rapidly with the emission of light) have been observed upon heating of alternating elemental thin films which have a large negative heat of mixing.[12] These reactions generally involve melting of one of the layers which removes the diffusion barriers formed by solid state reactions at the layer interfaces. Solid state reactions have been extensively studied using differential thermal analyses, and the nature and extent of compounds formed have been observed using high resolution electron microscopy in some systems.

Self-propagating high temperature synthesis of compounds from elemental powders (SHS) has been explored for making ceramic materials at atmospheric pressure.[13] These reactions are thermally initiated locally, and propagate

through the powder at rates typically on the order of a centimeter/s. Shock initiated reactions in powders differ from SHS and more conventional thermally initiated reactions in that they are initiated under high pressure and the initiation takes place throughout the powder in the time taken by the shock wave to traverse the sample.

Chapter 2 of this thesis presents studies of the formation of the intermetallic compound NiSi from the elemental powders. The uniform shock conditions, produced by the impact of a stainless steel flyer plate with the powder mixture held in a cylindrical steel cavity, permitted determination of the shock energy required to initiate the reaction. The initiation behavior was compared to thermal initiation at atmospheric pressure.

Chapter 3 of this thesis presents studies of the reaction forming  $\text{Ti}_5\text{Si}_3$  from the elemental powders. The heat of mixing for this reaction is approximately seven times greater than that for the reaction forming NiSi, while the melting temperature for the compound is  $2130^\circ\text{C}$  (vs.  $992^\circ\text{C}$  for NiSi). The thermal conductivity of Ti is about one-fourth of that of Ni. Shock conditions for initiation of the reaction were compared to the conditions for thermal initiation of the reaction at atmospheric pressure. The SHS behavior of the Ti and Si mixtures is compared to that of Ni and Si mixtures.

Chapter 4 presents a study of the consolidation of a metallic glass powder undertaken to produce bulk samples of the material for mechanical property measurements.

## REFERENCES

- [1] Y. B. Zel'dovich and Y. P. Raizer, "Physics of Shock Waves and High-Temperature Hydrodynamic Phenomena, Vols. I and II," Academic Press, San Francisco (1976).
- [2] "High Velocity Impact Phenomena," R. Kinslow (ed.), Academic Press, New York (1970).
- [3] C. A. Parsons, Phil. Trans. Roy. Soc., London A220, 67 (1920).
- [4] P. S. DeCarli and J. C. Jamieson, Science 133, 821 (1961).
- [5] R. A. Graham, B. Morosin, and B. Dodson, "The Chemistry of Shock Compression: A Bibliography," Sandia National Laboratories Report SAND 83-1887.
- [6] G. A. Adadurov, V. I. Gol'danskii, and P. A. Yampolskii, "Mendeleev Chemistry Journal 18, 92 (1973).
- [7] G. A. Adadurov and V. I. Gol'danskii, Russian Chemical Reviews 50, 948 (1981).
- [8] R. A. Graham, B. Morosin, Y. Horie, E. L. Venturini, M. Boslough, M. J. Carr, and D. L. Williamson, in "Shock Waves in Condensed Matter," Y. M. Gupta (ed.), Plenum Publishing Corporation, New York, 693 (1963).
- [9] R. A. Graham, J. Phys. Chem. 83, 3048 (1979).
- [10] "LASL Shock Hugoniot Data," S. P. Marsh (ed.), University of California Press, Los Angeles (1980).
- [11] R. B. Schwarz, P. Kasiraj, and T. Vreeland, Jr. in "Metallurgical Applications of Shock Waves and High-Strain-Rate Phenomena," L. E. Murr, K. P. Staudhammer, and M. A. Meyers (eds.), Marcel Dekker, New York, 313 (1986).
- [12] F. Bordeaux and A. R. Yavari, J. Mater. Res. 5, 1656 (1990).
- [13] W. F. Henshaw, A. Niiler, and T. Leete, ARBRL-MR-03354.

## 2. CALCULATION OF THE SHOCK HUGONIOT FOR MIXTURES

### 2.1 A Hugoniot theory for solid and powder mixtures

Barry R. Krueger and Thad Vreeland, Jr.

Keck Laboratory of Engineering Materials

California Institute of Technology, 138-78

Pasadena, CA 91125

#### ABSTRACT

A model is presented from which one can calculate the Hugoniot of solid and porous two component mixtures up to moderate pressures using only static thermodynamic properties of the components. The model does not presuppose either the relative magnitude of the thermal and elastic energies or temperature equilibrium between the two components. It is shown that for a mixture, the conservation equations define a Hugoniot surface and that the ratio of the thermal energy of the components determines where the shocked state of the mixture lies on this surface. This ratio, which may strongly affect shock initiated chemical reactions and the properties of consolidated powder mixtures, is found to have only a minor effect on the Hugoniot of a mixture. It is also noted that the Hugoniot of solids and solid mixtures is sensitive to the pressure derivative of the isentropic bulk modulus.

#### INTRODUCTION

The Hugoniot of a mixture is intimately related to the current interest in shock initiated chemical reactions.[1-5] With the high temperature and pressure associated with shock wave processing, it may be possible to concurrently synthesize and form near net shape parts of intermetallic compounds and other materials. Shock processing is potentially a viable technology for producing composite

materials in which it is necessary to control chemical reactions between the matrix and reinforcing powders since such reactions often have deleterious effects on the mechanical properties of the composite.

Fully understanding shock initiated chemical reactions and shock compaction of composites is dependent upon knowing the Hugoniot of the mixture of interest. To this end, several models have been put forth. A popular approach has been developed by McQueen et al.[6] Their theory requires the Hugoniots of the components and assumes the thermal energy of a shocked mixture to be small compared to the elastic energy. This assumption is necessary since their model does not account for a difference in the temperature rise of the components which will occur in shocked solid and particularly powder mixtures. Duvall and Taylor [7] have used a mixture method that relies on knowing the component's Gibb's free energy, and they assume the components to be in thermal equilibrium.

Both of these approaches assume conditions not necessarily valid in the shock state. In shocked porous media the relative magnitude of the thermal and elastic energy is just the opposite of McQueen's assumption. The difference in temperature of the two components of a mixture may be large,[8] and in many materials will not equilibrate quickly relative to the shock rise time.[7] In light of this, we have developed a formulation which allows for large thermal energies and does not require either thermal equilibrium between components or a large ratio of elastic to thermal energy. This calculation employs a simple Hugoniot theory based on the Mie-Grüneison equation of state and a linear relation for the isentropic compressibility as a function of pressure. It is sufficient to allow discussion of the effect of energy partitioning between components of a powder mixture. More sophisticated equations of state for solids have been developed [9-11] and discussed [12], but are somewhat less amenable to the mixed media Hugoniot formulation.

## PRELIMINARY DISCUSSION

For the proposed Hugoniot theory of a two component mixture, two preliminary assumptions are made:

- (i) the components are at equal pressures.
- (ii) the components have equal particle velocities.
- (iii) chemical energy is not released during the shock rise time.

Assumption (i) is justified as follows. If the pressures were initially different, equilibration would occur within a few multiples of a time  $t = d/c_0$ , where  $d$  is an average particle diameter and  $c_0$  is the compressive sound velocity.[7] For example, in copper  $c_0$  is on the order of  $5 \times 10^3$  m/sec. A powder size of  $100 \mu\text{m}$  gives a characteristic pressure equilibration time of approximately 100 nsec. This is on the order of the shock rise time measured in ductile powders [13] indicating that pressure equilibration will occur in a time scale similar to the shock rise time. The time required to establish a well-defined pressure in the shock state may be considered a definition of the rise time.

The second assumption, that the components have equal particle velocities behind the shock, is based on experimental evidence. In shock compaction experiments on 1:1 atomic percent Ni/Si, Ni/Ti and Ni/Cu powders, we see no evidence that the components maintain different particle velocities. If this were true, the lower shock impedance material would segregate in the shock direction which is not observed. There is also no known experimental evidence in the literature that the two components of a mixture maintain different particle velocities, although differences in particle velocities have been used to explain some shock initiated chemical reactions.[3]

The third assumption, excluding consideration of chemical energy, is generally valid given the relative slowness of diffusional transport to sound velocity. In systems subject to chemical reactions, it has been shown that the reactions may

initiate within the shock front in ultra-fine powders.[14] If extensive reactions do occur within the shock rise time, the present model is not applicable.

Assumptions (i) and (ii), together with conservation of mass, momentum, and energy, imply that the two components absorb different amounts of energy and are therefore, in general, at different average temperatures immediately behind the shock front. An example supporting the implied energy partitioning is the theoretical and experimental work on the shock consolidation of Al/SiC metal matrix composites from Al and SiC rods, (i.e., two dimensional powders).[8] Further evidence is shown in Figure 1 which is a micrograph of a shock consolidated mixture of hard and soft maraging steel powders heat treated to VH 620 and 280, respectively. The softer, light etching particles have deformed significantly in comparison with the harder particles. Intuitively, in a mixture of soft and hard, small and large or irregular and regularly shaped particles, one would expect the former to absorb more energy than the latter which will result in different average particle temperatures behind the shock.

A simple argument reveals that for typical powders, a temperature difference will not equilibrate quickly, but in fact, orders of magnitude more slowly than any pressure difference. Significant thermal conduction will occur over distances  $d = \sqrt{\kappa t}$ , where  $\kappa$  is some average thermal diffusivity. Using typical parameters of  $d = 100 \mu\text{m}$  and the thermal diffusivity of a good thermal conductor such as Cu indicates that temperature differences will equilibrate 2 to 3 orders of magnitude more slowly than pressure differences and in a time which may be longer than the shock duration itself.[7] Obviously, the temperature must be continuous across the particle boundaries of the two components, but the proposed theory is a bulk thermodynamic model which considers average component temperatures.

If the particle size is approximately 100 nm or smaller, the difference between pressure and temperature equilibration times becomes small, and the

equilibration times are on the order of the shock rise time. This effect has been exploited by Boslough in his measurements of shock temperatures in thermitite and other systems using radiation pyrometry.[14,15] The theory presented here can treat ultra-fine particle shock consolidation by assuming a thermal energy ratio such that the components are at equal temperatures as will be explained below.

## THEORY

With the assumptions discussed above, the laws of conservation of mass, momentum and energy will be no different for a mixture provided that no chemical reactions occur:

$$(1) \quad \rho_{00AB} C_S = \rho_{1AB} (C_S - u_1) \quad \text{Conservation of Mass.}$$

$$(2) \quad P_1 - P_0 = \rho_{00AB} C_S u_1 = \rho_{1AB} (C_S - u_1) u_1 \quad \text{Conservation of Momentum.}$$

$$(3) \quad \rho_{00AB} C_S \left[ E_1 - E_0 + \frac{1}{2} u_1^2 \right] = P_1 u_1 \quad \text{Conservation of Energy.}$$

where the  $\rho_{00AB}$  is the initial density of the mixture;  $\rho_{1AB}$  is the shocked density;  $C_S$  is the shock velocity;  $u_1$  is the particle velocity;  $P_0$  is the initial pressure;  $P_1$  is the shock pressure, and  $E_0$  and  $E_1$  are the initial and final specific internal energy of the mixture, respectively. Substituting (1) and (2) into (3) and dividing the specific internal energy between the two components gives:

$$(4) \quad x \Delta E_A + (1-x) \Delta E_B = \frac{1}{2} P_1 \left[ V_{00AB} - V_{1AB} \right],$$

where  $x$  is the mass fraction of material A;  $V_{00AB}$  and  $V_{1AB}$  are the initial and shocked specific volumes of the mixture, respectively.  $\Delta E_A$  and  $\Delta E_B$  are the

changes in specific internal energy of the two components, and the initial pressure is assumed to be zero. Equation (4) is a simple expansion of the familiar equation  $E = \frac{1}{2}P[V_{00} - V_1]$ . The  $\Delta$ 's can be removed if the ambient energy is used as a reference.

The energy and pressure of each constituent can be separated into thermal and elastic (isentropic) components,

$$(5) \quad E_A = E_{TA} + E_{EA} \quad , \quad E_B = E_{TB} + E_{EB},$$

$$(6) \quad P_A = P_{TA} + P_{EA} = P_B = P_{TB} + P_{EB},$$

where the E and T subscripts refer to the elastic and the thermal components, respectively. The second equality in (6) is due to the equal pressure assumption. Using the definition of the Grüneisen parameter  $\gamma \equiv V(\partial P/\partial E)_V$  and assuming each component's Grüneisen parameter to volume ratio is constant and temperature independent, the thermal pressure in terms of the thermal energy of the two components becomes:

$$(7) \quad dP_{TA} = \frac{\gamma_A dE_{TA}}{V_A} \approx \frac{\gamma_{0A} dE_{TA}}{V_{0A}} \Rightarrow P_{TA} = \frac{\gamma_{0A} E_{TA}}{V_{0A}},$$

$$dP_{TB} = \frac{\gamma_B dE_{TB}}{V_B} \approx \frac{\gamma_{0B} dE_{TB}}{V_{0B}} \Rightarrow P_{TB} = \frac{\gamma_{0B} E_{TB}}{V_{0B}}.$$

This is a simpler assumption than that applied by Jeanloz.[12] Equations (5)–(7) can be substituted into (4) yielding:

$$(8) \quad P_1 = \frac{\sigma_A P_{EA}(\lambda_A) + \sigma_B P_{EB}(\lambda_B) - \frac{x E_{EA}(\lambda_A)}{V_{0A} V_{0B}} - \frac{(1-x) E_{EB}(\lambda_B)}{V_{0A} V_{0B}}}{\sigma_A + \sigma_B - \frac{1}{2}[\varphi - \eta_A \lambda_A - \eta_B \lambda_B]},$$

where

$$\sigma_A = \frac{x}{\gamma_{0A} V_{0B}}, \quad \sigma_B = \frac{(1-x)}{\gamma_{0B} V_{0A}}, \quad \eta_A = \frac{x}{V_{0B}}, \quad \eta_B = \frac{(1-x)}{V_{0A}},$$

$$\lambda_A = \frac{V_{1A}}{V_{0A}}, \quad \lambda_B = \frac{V_{1B}}{V_{0B}}, \quad \varphi = \frac{V_{00AB}}{V_{0A} V_{0B}}.$$

$V_{1A}$  and  $V_{1B}$  are the shocked specific volumes of the A and B components, respectively. The volume dependence ( $\lambda_i$ ) of the elastic pressures and energies is indicated, and hydrodynamic material behavior is assumed. The distension of the powder,  $m \equiv V_{00AB}/V_{0AB}$  where  $V_{0AB}$  is the solid volume of the mixture at standard conditions, enters equation (8) through the parameter  $\varphi$ .

Next, one must choose expressions for the elastic pressures and energies. By assuming a linear dependence of the isothermal bulk modulus with pressure, Murnaghan [16] derived the equation:

$$(9) \quad P_E = \frac{\beta_{0T}}{\beta'_{0T}} \left[ \left[ \frac{V_0}{V_1} \right]^{\beta'_{0T}} - 1 \right] = \frac{\beta_{0T}}{\beta'_{0T}} \left[ \lambda^{-\beta'_{0T}} - 1 \right]$$

where  $\beta_{0T}$  is the isothermal bulk modulus at standard conditions, and  $\beta'_{0T}$  is its first derivative with respect to pressure at constant temperature. Anderson [18] has shown that (9) is a good approximation over a wide range of materials and to volume ratios of around 0.8. However, the elastic pressure in the shock process is not isothermal but rather isentropic. Integrating at constant entropy, a linear relationship between the isentropic bulk modulus and pressure yields a similar equation,

$$(10) \quad P_E = \frac{\beta_{0S}}{\beta'_{0S}} \left[ \left[ \frac{V_0}{V_1} \right]^{\beta'_{0S}} - 1 \right] = \frac{\beta_{0S}}{\beta'_{0S}} \left[ \lambda^{-\beta'_{0S}} - 1 \right],$$

where  $\beta_{0S}$  is the isentropic bulk modulus at standard conditions, and  $\beta'_{0S}$  is its first derivative with respect to pressure at constant entropy. Then, (10) can be integrated to get the elastic energy. It is typically derived from ultrasonic measurements. Under moderate pressures and non-cryogenic temperatures,  $\beta'_{0S}$  at constant entropy and  $\beta'_S$  at constant temperature will be similar (within 0.1%) for most materials.[17] It has been assumed that  $\left[\frac{\partial\beta_S}{\partial P}\right]_S \equiv \beta'_S \approx \left[\frac{\partial\beta_S}{\partial P}\right]_T$  which has been determined for many substances using static pressure sound velocity measurements.[17,18] To examine the reliability of the model in a variety of materials, it has been assumed that  $\beta'_S \approx \left[\frac{\partial\beta_T}{\partial P}\right]_T$ , and  $\left[\frac{\partial\beta_T}{\partial P}\right]_T$  was calculated from equation of state data.[19] According to Anderson's data, the value of the two approximations for  $\beta'_S$  do not differ greatly.

Note that (8) is valid for all porosities since no assumptions were made in its derivation concerning the relative magnitude of the thermal and elastic energy components except that the ratio  $\gamma/V$  is constant and independent of temperature. Oh [20] has shown that the constant  $\gamma/V$  approximation is inaccurate at very high energies, however this discrepancy has been allowed since most shock compaction and shock initiated reaction experiments are conducted at moderate energies.

Equation (8) gives the shock pressure in terms of the two component's volumes. For a single material, the shocked volume is determined as a function of pressure. Then, this equation together with the equation  $u_1 = \sqrt{P\Delta V}$  and a known flyer pressure-particle velocity relationship can be used to determine all the shock parameters. However since (8) gives the pressure in terms of both volumes, there is one more unknown parameter. In other words, (8) is a Hugoniot surface which

depends on the individual volumes of the components rather than simply the total shocked volume.

Since there exists one more unknown, we initially considered measuring one more shock parameter, specifically the shock velocity since it lends itself easily to measurement. With a known shock velocity, (1), (2), (8) together with (9) and a known flyer pressure-particle velocity relationship constitute a system of four equations with four unknowns,  $P_1$ ,  $u_1$ ,  $V_{1A}$ , and  $V_{1B}$ . Once the unknowns are determined, (6), (7) and (10) can be used to determine the thermal energy of the two components and hence their temperatures.

Calculations show that small variations (a few percent) of the shock speed away from the value calculated assuming averaged properties may lead to nonphysical results such as a negative thermal energy for one of the components. Therefore, the theory predicts the shock velocity in a mixture is near the shock velocity assuming averaged properties and that any difference will probably be smaller than the resolution of a shock speed measurement. Another approach is to assume the shock speed is the value calculated using averaged properties. This results in calculated energy partitioning which is non-intuitive and contradicts experiments in certain powder mixtures such as TiAl-6V-4 and SiC where the very hard SiC deforms relatively little while the Hugoniot assuming a shock velocity calculated from averaged properties predicts that it absorbs significant thermal energy.

A third approach is to obtain a fifth equation by recognizing that at given shock conditions, there exists a thermal energy partitioning ratio which is determined by the relative mechanical properties, sizes and shapes of the two components. The softer, smaller and irregularly shaped component absorbs more thermal energy, or if one wished to assume equal temperatures, as in the case of ultra-fine powders, it is possible to determine an approximate thermal energy ratio

based on the specific heats of the components over some expected temperature range. Except for the last case, quantitatively predicting the thermal energy partitioning for a given mixture is difficult. Nevertheless, at given shock conditions, there does exist a thermal energy ratio of the form:

$$(11) \quad \xi(P_1, C_S, u_1) \equiv E_{TB}/E_{TA}.$$

Using equations (6), (7) and (11), we obtain the equation,

$$(12) \quad P_1 \left(1 - \frac{\xi}{\epsilon}\right) = P_{EB}(\lambda_B) - \frac{\xi}{\epsilon} P_{EA}(\lambda_A), \quad \text{where } \epsilon = \frac{V_{0B} \gamma_{0A}}{V_{0A} \gamma_{0B}}.$$

Equations (1), (2), (8), (12) and a known flyer pressure–particle velocity relationship constitute a system of five equations and five unknowns,  $C_S$ ,  $P_1$ ,  $u_1$ ,  $V_{1A}$ , and  $V_{1B}$  which can be solved numerically.

To determine the effects of thermal energy partitioning on a mixture's Hugoniot, we have assumed the simplest possible form for (11),  $\xi = \text{constant}$ . Doing so simplifies the calculations, but more importantly, assuming  $\xi$  is constant includes the extreme possibility that one component absorbs no thermal energy (i.e.,  $\xi = 0$  or  $\infty$ ).

## VALIDATION OF THE MODEL FOR HOMOGENEOUS MATERIALS

To test the model, the Hugoniots of solid single component materials were calculated. As discussed earlier, this is the degenerate case of a two component mixture, and defining a thermal energy ratio is not necessary. The materials were chosen based on the the availability of thermodynamic data to approximate  $\beta'_S$  and the availability of statistically significant Hugoniot data over a range of compression where a first order thermal expansion of a material's isentropic bulk modulus is

expected to be valid. The materials and the thermodynamic data used are shown in Table I.

A result of the calculations is that the  $C_s - u_1$  relationship is nearly linear as is found experimentally. For all the calculated single component Hugoniot, the correlation coefficient between  $C_s$  and  $u_1$  is greater than 0.995. Therefore, the proposed model qualitatively fits the experimental Hugoniot data. The results are shown in Table II in the form  $C_s = A + B*u_1$  along with the values of A and B determine from a linear regression fit of the experimental data [21] over the velocity ranges indicated. As can be seen in Table II, the calculated shock intercepts match the experimental values well. The average absolute difference between the calculated and experimental values is only 59 m/sec. However, the calculated particle velocity coefficients are consistently higher than the experimental values with an average difference of 14.4%.

By varying the thermodynamic parameters within a reasonable range of uncertainty, it was determined that the calculated particle velocity coefficients are sensitive to  $\beta'_s$ . This is consistent with the result of Ruoff,[24] who derived  $B = (\beta'_s + 1)/4$  from the Murnaghan expression, formula (10).

The Hugoniot of the solids in Table I were recalculated with the same parameters except for  $\beta'_s$ , which were adjusted so the calculated particle velocity coefficients fit the experimental values. Table III shows the values of  $\beta'_s$  necessary to fit the experimental particle velocity coefficients and the ratio of the fitted value to the original estimate. This ratio lies between .69 and .91 and roughly varies inversely with the material's bulk modulus. Also shown are the new values of the calculated shock intercept which differ little from the values calculated originally and the experimental values.

These comparisons of calculated and experimental data show that the model qualitatively fits experimental solid Hugoniot using estimates of  $\beta'_s$  and that the values of  $\beta'_s$  can be varied so that the calculated solid Hugoniot fit the experimental data better. This is not strictly correct, but can be used as an approximation strategy when the Hugoniot and thermodynamic data are both available.

The data necessary for a comparison between experimental and calculated results for porous materials is available for Cu. The Hugoniot of this powder was calculated with the value of  $\beta'_s$  used to fit the experimental solid Hugoniot particle velocity coefficients, however it should be noted that the results change by no more than five percent and usually less than 2 percent by using the original estimate of  $\beta'_s$  since the elastic energy in a shocked powder is only a small fraction of the total energy. For this reason, the formulation derived here is expected to be most applicable to porous media. As can be seen in Table IV, the calculated values of both the shock intercept and particle velocity coefficient match the experimental data well.

The comparison between calculated and experimental Hugoniot in Table IV shows that the theory can quantitatively determine the Hugoniot of a distended single component material. It is important to emphasize that small variations in  $\beta'_s$  do not greatly affect the calculated Hugoniot for a distended media. This, together with the results discussed for solid materials, shows that the model accurately describes a porous material's shock response. This implies that the extension of the model to a porous mixture should be sufficiently accurate to make certain conclusions about a mixture's Hugoniot since the physical description of a material's shock response is the same in the full two component theory. In the following section, the Hugoniot of mixtures of the materials in Table I are discussed.

## APPLICATION TO MIXTURES AND DISCUSSION

For the following calculations, properties were averaged volumetrically using the Reuss averages for the elastic properties:

$$(13) \quad V_{0AB} = \sum_i x_i V_i,$$

$$(14) \quad \left[ \frac{V}{\gamma} \right]_{0AB} = \sum_i x_i \left[ \frac{V}{\gamma} \right]_{0i},$$

$$(15) \quad \beta_{0SAB} = V_{0AB} \left[ \sum_i \frac{x_i V_{0i}}{\beta_{0Si}} \right]^{-1},$$

$$(16) \quad \beta'_{0SAB} = \left[ \frac{\beta_{0SAB}^2}{V_{0AB}} \sum_i x_i V_{0i} \left[ \frac{1 + \beta'_{0Si}}{\beta_{0Si}^2} \right] \right] - 1.$$

Unfortunately, few Hugoniot of well characterized mixtures have been determined experimentally over a range of composition. There is sufficient data for a comparison with slightly distended mixtures of sintered W infiltrated with 24 and 45 wt.% Cu.[22] The calculated and experimental results for W – 24 wt.% Cu are shown as  $C_s$  vs.  $u_1$  plots in Figure 2. The three curves correspond to the Hugoniot calculated assuming averaged properties and the extreme cases in which the W or Cu absorb no thermal energy. A good fit to data is the calculated Hugoniot where the W absorbs no thermal energy which is closer to what one might expect, however, this conclusion is poorly supported since the Hugoniot assuming the opposite extreme also fits the data well and better than the calculated Hugoniot assuming averaged properties.

Interestingly, the calculated Hugoniot are non-linear at low particle velocities. The linearity of the  $C_s - u_1$  relationship in solid materials is well-known.[23,24] Some evidence of curvature in the relationship in distended solids exists for sintered aluminum and copper.[25] Although the number of experimental points is small, the data is well fit by the non-linearity. All three of the calculated Hugoniot fit the non-linearity well, however little difference is expected in this range because the thermal energy is smaller at lower particle velocities. McQueen et al.[6] supposed, by comparison with experimental single component porous Hugoniot, that the curvature is due to the initial porosity of the samples. Calculations assuming no initial porosity do show the  $C_s - u_1$  relationship to be linear, thereby confirming this conclusion, however since our model assumes hydrodynamic material behavior and matches the curvature in the experimental data, it can be concluded that the curvature is not the result of material rigidity effects.

The calculated Hugoniot for W – 45 wt.% Cu is linear over the range of particle velocities investigated which was higher than in the previous case due to the lack of experimental data at lower particle velocities. The calculated values of A and B are 3.108 km/sec and 2.014 respectively, assuming averaged properties, 3.125 km/sec and 1.917 respectively, assuming the Cu absorbs no thermal energy and 3.137 and 1.954 respectively, assuming the W absorbs no thermal energy. The values of A and B determined from the experimental data over the particle velocities 189 m/sec to 878 m/sec are 3.003 and 2.021, respectively. It should be noted that one experimental data point was excluded because the density of that particular sample was significantly lower. The calculated values of A and B assuming mass averaged properties are very close to the experimental values. As with the other W–Cu mixture, the two extreme Hugoniot lie on the same side of the Hugoniot calculated assuming average properties in the  $C_s - u_1$  plane.

The Hugoniot of several other mixtures, listed in Table V, have been calculated to investigate the effects of the thermal energy partitioning ratio on the Hugoniot although no experimental data is available for these systems. The weight fraction of the components was taken to be 50% and the distension to be 1.5. It was assumed that a 304 stainless steel flyer was impacting the sample at velocities from 800 to 2000 m/sec. These systems were chosen because they represent a wide range of possible mixtures, and the shock conditions were chosen because they are typical of shock compaction and shock initiated reaction experiments. The results are shown in Table V in the form  $C_s = A + B(u_1)$ . The results for the Mg/Au system when the Mg absorbs no thermal energy have been excluded because the calculated volume of Au was found to be unrealistically high.

One observation drawn from Table V is that unlike the W - Cu system, the Hugoniot in the  $C_s - u_1$  plane assuming that one component absorbs no thermal energy straddle the Hugoniot assuming averaged properties. Also unlike the W-24 wt% Cu mixture, the  $C_s - u_1$  relationships are highly linear. The Hugoniot of these mixtures may be non-linear at lower particle velocities with finite distensions, however these possibilities were not explored.

Another observation is that in a system where one would expect the thermal energy of one component to be nearly zero, it appears possible to experimentally determine  $\xi$  in equation (11), however there would be many difficulties in such experiments. First, the calculations have assumed  $\xi$  to be constant. It is unlikely that  $\xi$  will remain constant over a wide range of shock conditions. More significantly, the resultant effect on the macroscopic shock parameters is relatively small. For example, the largest difference found between an extreme Hugoniot and a Hugoniot assuming averaged properties occurs in the Cd/Nb system. This translates into a difference of 4.7%, 6.3%, 8.8%, 2.4% and 8.8% in total energy, pressure, shock velocity, particle velocity and total thermal energy, respectively at

the highest impact velocity. The difference in the total elastic energy is 52% in this case which may be important in systems with, for example, pressure induced phase transitions, however in general, this is not as significant as it may seem since the total elastic energy, assuming average properties, is only 7.7% of the total energy deposited. In the other systems and with lower projectile velocities, the percentage difference in the macroscopic shock parameters is smaller and typically less than 3%. Therefore to determine  $\xi$ , a large number of carefully conducted experiments would be required to get statistically significant results, and even then, a small error in the measured shock parameters would result in a large uncertainty in  $\xi$ .

Since the above calculations are for extremes in thermal energy partitioning and a wide range of possible mixtures have been investigated, it appears that a Hugoniot assuming averaged properties is a valid approximation to the Hugoniot of a mixture under the typical conditions of a shock compaction or shock initiated reaction experiment even though the thermal energies, and hence temperatures, of the components may differ significantly. Therefore, equations (13) – (16) can be used to determine the averaged properties and equations (1), (2), the flyer pressure–particle velocity relationship and a reduced form of equation (8) can be used to calculate the shock parameters for a given flyer velocity. Unfortunately, if a mixture's distension is close or equal to 1, the solid Hugoniots of the components need to be known to determine  $\beta'_s$  until further theoretical or experimental work is done, but in porous mixtures an estimate of  $\beta'_s$  is sufficient since the elastic energy is relatively small.

## CONCLUSIONS

A theory has been presented to determine the Hugoniot of solid and powder two component mixtures using only static pressure data. In developing the model, it was assumed that the pressures and particle velocities of the components were

equal while no assumptions were made regarding the relative magnitude of the thermal and elastic energies or temperature equilibrium between the components. The validity of the equal pressure assumption and the fact that temperature equilibrium will not be reached immediately behind the shock front was argued in terms of characteristic equilibration times. The equal particle velocity assumption is based on experimental evidence. In addition, it was assumed that significant amounts of chemical energy are not released during the shock wave rise time.

The model was shown to qualitatively fit the solid Hugoniot of single component materials using approximations to  $\beta'_S \equiv \left[ \frac{\partial \beta_S}{\partial P} \right]_S \approx \left[ \frac{\partial \beta_S}{\partial P} \right]_T \approx \left[ \frac{\partial \beta_T}{\partial P} \right]_T$ . Furthermore, the experimental data could be better fitted by adjusting  $\beta'_S$ . Using the values of  $\beta'_S$  fitted to the experimental data, it was shown that the calculated Hugoniot of distended single component materials fit experimental data well, Approximations to  $\beta'_S$  are adequate for porous materials since thermal energy greatly exceed elastic energy.

The relatively simple Reuss averages were used for the bulk moduli of the composite mixtures. More complex methods for bounding the elastic properties of mixtures could be applied,[27] but we do not believe that they would change the conclusions which follow.

The mixture Hugoniot model was compared to experimental Hugoniot data in the W–Cu system. The calculated Hugoniot for this system were interesting in that the Hugoniot assuming either the W or Cu absorb no thermal energy lie on the same side of the Hugoniot calculated using averaged properties in the  $C_S - u_1$  plane. An interesting feature of the data for slightly distended W–Cu with 24 wt.% Cu is the non-linear  $C_S - u_1$  relationship. This non-linearity is well-fit by the Hugoniot model. The model fits the non-linearity as a result of a small initial porosity.

A series of calculations were then performed on mixtures of materials under typical shock compaction and shock initiated reaction conditions. It was shown that extreme changes in the thermal energy ratio did affect the Hugoniot, however it was argued that the resultant effect on the macroscopic shock parameters is relatively small and would be difficult to determine experimentally. Given this result, it can be concluded that a Hugoniot calculated with equations (1), (2), a reduced form of (8) and the known flyer pressure—particle velocity relationship and assuming averaged properties using equations (13) – (16), is a reasonable approximation for determining the total energy, pressure, thermal energy etc. of a shocked mixture regardless of the component thermal energy ratio, and an accurate approximation for a porous mixture. This indicates that the thermal energy partitioning ratio, which will have an important effect on the shock compaction and shock initiated reaction processes, will need to be determined by experimental and theoretical means other than by measuring macroscopic shock parameters.

#### ACKNOWLEDGEMENTS

We would like to thank Andrew Mutz for Figure 1 and his work on the maraging steel experiment. We would also like to thank Ricardo Schwarz of Los Alamos National Laboratories for helpful conversations and his thoughtful insight. This work was supported under the National Science Foundation's Materials Processing Initiative Program, Grant No. DMR 8713258.

## REFERENCES

- [1] M. B. Boslough, in "Proceedings of the Ninth Symposium (International) on Detonation," (In press, 1990).
- [2] M. B. Boslough, *J. Chem. Phys.* 92, 3, 1839 (1990).
- [3] S. S. Batsanov, G. S. Doronin, S. V. Klochdov, and A. I. Teut, in "Combustion, Explosions and Shock Waves," 22, 765 (1986).
- [4] R. A. Graham, B. Morison, Y. Horie, E. L. Venturini, M. B. Boslough, M. Carr, and D. L. Williamson, in "Shock Waves in Condensed Matter," Y. M. Gupta (ed.), Plenum Press, New York, 693 (1986).
- [5] N. N. Thadhani, M. J. Costello, I. Song, S. Work, and R. A. Graham, in "Proceedings of the TMS Symposia on Solid State Powder Processing," Indianapolis, (October 1–4, 1989), to be published.
- [6] R. G. McQueen, S. P. Marsh, J. N. Taylor, J. N. Fritz, and W. J. Carter, in "High Velocity Impact Phenomena," R. Kinslow (ed.), Academic Press, New York, 293 (1970).
- [7] G. E. Duvall, and S. M. Taylor, Jr., *J. Composite Materials* 5, 130 (April, 1971).
- [8] R. L. Williamson, R. N. Wright, G. E. Korth, and B. H. Rabin, *J. Appl. Phys.* 66, 1826 (1989).
- [9] R. Grover, I. C. Getting, and G. C. Kennedy, *Phys. Rev. B.* 7, 567 (1973).
- [10] S. Eliezer, A. Garak, and H. Hora, "An Introduction to Equations of State: Theory and Practice," Cambridge, New York, (1986).
- [11] P. Vinet, J. Ferrante, J. R. Smith, and J. H. Rose, *J. Phys. C* 19, 467 (1986).
- [12] R. Jeanloz, *J. Geogh. Res.* 94, 5873 (1989).
- [13] R. B. Schwarz, P. Kasiraj, and T. Vreeland, Jr., in "Metallurgical Applications of Shock Waves and High-Strain-Rate Phenomena," L. E. Murr, M. A. Meyers and K. Staudhammer (eds.), Marcel Dekker, New York, 313 (1986).

- [14] M. B. Boslough, and R. A. Graham, Chem. Phys. Lett. 121, 446 (1985).
- [15] M. B. Boslough, J. Chem. Phys. 92, 1839 (1990).
- [16] F. D. Murnaghan, Proc. Nat'l. Acad. Sci. 30, 244 (1944).
- [17] G. Simmons and H. Wang, in "Single Crystal Elastic Constants and Calculated Aggregate Properties: A Handbook," MIT, London, 295 (1971).
- [18] O. L. Anderson, J. Phys. Chem. Solids 27, 547 (1966).
- [19] V. N. Zharkov and V. A. Kalinin, "Equations of State for Solids at High Pressures and Temperatures," Consultants Bureau, New York (1971).
- [20] K. Oh and P. Persson, J. Appl. Phys., submitted.
- [21] P. E. Marsh (ed.), "LASL Shock Hugoniot Data," University of California Press, Berkeley (1980).
- [22] See Reference #18, 523 and 525.
- [23] B. J. Adler, in "Solids Under Pressure," W. Paul and D. W. Warschauer (eds.), McGraw-Hill, New York (1963).
- [24] A. L. Ruoff, J. Appl. Phys. 38, 4976 (1967).
- [25] See Reference #18, 177 and 64.
- [26] D. Lazarus, Phys. Rev. 76, 4 (1949).
- [27] J. P. Watt, Rev. Geophys. and Space Phys. 14, 541 (1986).

Table I. Materials and thermodynamic data used to calculate single material Hugoniot. Most data is derived from equation of state data from [19]. Data for copper is from [26]. Data in [17] is similar.

Material	Density (g/cm <sup>3</sup> )	$\beta_s$ (GPa)	$\beta'_s$	$\gamma_0$
Cu	8.94	139.76	4.994	2.04
Zn	7.14	65.40	5.421	2.38
Nb	8.60	175.40	3.551	1.69
Au	19.24	179.50	5.270	3.05
Pd	11.95	189.00	5.655	2.18
Co	8.82	194.60	4.700	1.99
W	19.20	308.10	3.996	1.54
Cd	8.64	48.57	7.015	2.20
NaCl	2.16	24.70	5.270	1.57
Mg	1.74	35.58	4.050	1.50
Ag	10.50	108.70	5.660	2.46
Ni	8.90	192.50	4.620	1.91
Pb	11.34	46.36	4.350	2.78

Table II. Results of Hugoniot calculations for single components materials.

Experimental values of A and B are taken from linear fits to data in [21].

Material	$u_1$ (min) (m/sec)	$u_1$ (max) (m/sec)	A Exp. (km/sec)	A Calc. (km/sec)	B Exp.	B Calc.
Cu	350	1324	3.898	3.918	1.526	1.632
Zn	588	1237	3.040	2.989	1.539	1.765
Nb	490	1038	4.514	4.478	1.127	1.256
Au	342	680	3.058	3.016	1.568	1.759
Pd	431	1416	3.963	3.944	1.611	1.792
Co	471	946	4.709	4.664	1.381	1.544
W	340	1156	4.008	3.975	1.278	1.361
Cd	572	1181	2.389	2.394	1.733	2.040
NaCl	326	1746	3.488	3.361	1.309	1.658
Mg	876	1935	4.620	4.459	1.180	1.398
Ag	471	987	3.262	3.183	1.570	1.818
Ni	475	987	4.656	4.698	1.355	1.520
Pb	263	890	2.042	1.976	1.446	1.574

Table III. Values of  $\beta'_S \equiv \beta'_{S\text{Fit}}$  required to fit experimental particle velocity coefficients. The very simple constitutive relationship results in the relatively large differences between measured and best-fit values of  $\beta'_S$ . Experimental values of A are taken from linear fits to data in [21].

Material	$\beta'_{S\text{Fit}}$	$\beta'_{S\text{Fit}}/\beta'_S$	A Exp. (km/sec)	A Calc. (km/sec)
Cu	4.525	0.906	3.898	3.912
Zn	4.340	0.801	3.040	2.963
Nb	3.025	0.852	4.514	4.476
Au	4.450	0.844	3.058	3.010
Pd	4.830	0.854	3.963	3.930
Co	4.025	0.856	4.709	4.660
W	3.650	0.913	4.008	3.973
Cd	5.380	0.767	2.389	2.345
NaCl	3.630	0.689	3.488	3.329
Mg	3.100	0.765	4.620	4.435
Ag	4.550	0.804	3.262	3.166
Ni	3.940	0.853	4.656	4.614
Pb	3.750	0.862	2.042	1.968

Table IV. Results of Hugoniot calculations for distended copper. Experimental values of A and B are taken from linear fits to data in [21].

Material	$u_1(\text{min})$ (m/sec)	$u_1(\text{max})$ (m/sec)	A Exp. (km/sec)	A Calc. (km/sec)	B Exp.	B Calc.
Cu						
m=1.13	610	1789	2.092	2.155	2.084	2.059
m=1.41	730	2018	0.718	0.805	2.208	2.166
m=1.57	769	2112	0.548	0.469	2.105	2.130

Table V. Results of mixture Hugoniot calculations

System (1/2)	Mass Averaged		Therm. En. 1=0		Therm. En. 2=0	
	A (km/sec)	B	A (km/sec)	B	A (km/sec)	B
Cu/Nb	0.345	2.378	0.337	2.372	0.281	2.472
Mg/Au	0.595	2.006	....	....	0.593	2.012
Cd/W	0.393	2.331	0.399	1.991	0.299	2.385
Co/Zn	0.362	2.331	0.177	2.692	0.383	2.221
Cd/Nb	0.394	2.219	0.391	2.151	0.210	2.631
NaCl/W	0.612	1.861	0.631	1.702	0.598	1.987

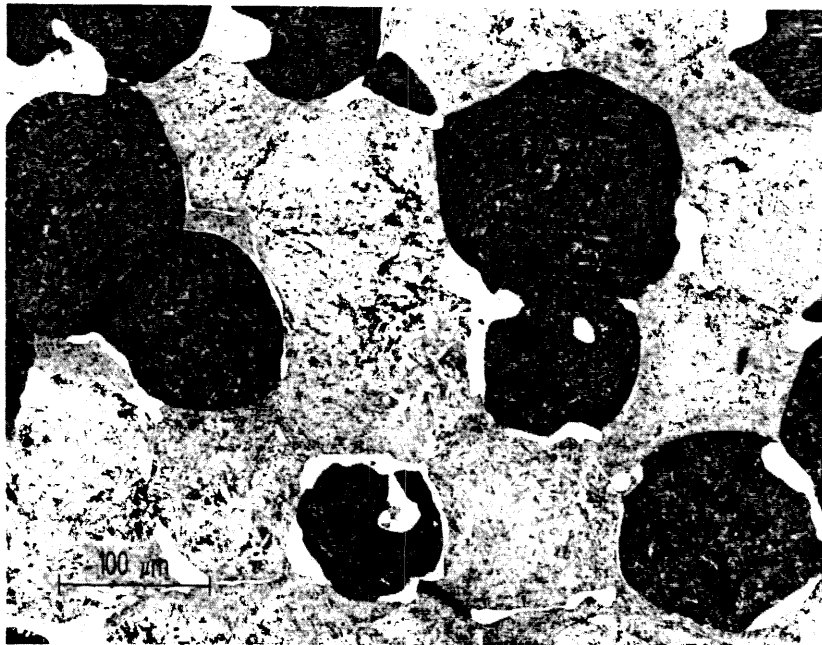


Figure 1. Shock consolidated  $-100 +200$  mesh maraging steel powders. The dark and light particles had a pre-shocked vickers microhardness of 280 and 640, respectively. The initial porosity was 32.0%. The 50/50 hard to soft mixture was impacted by a 304 stainless steel flyer at 986 m/sec. The soft particles deformed significantly compared to the hard particles as can be seen by the concavity of the interfaces. The very light material at the interfaces is rapidly quenched material:

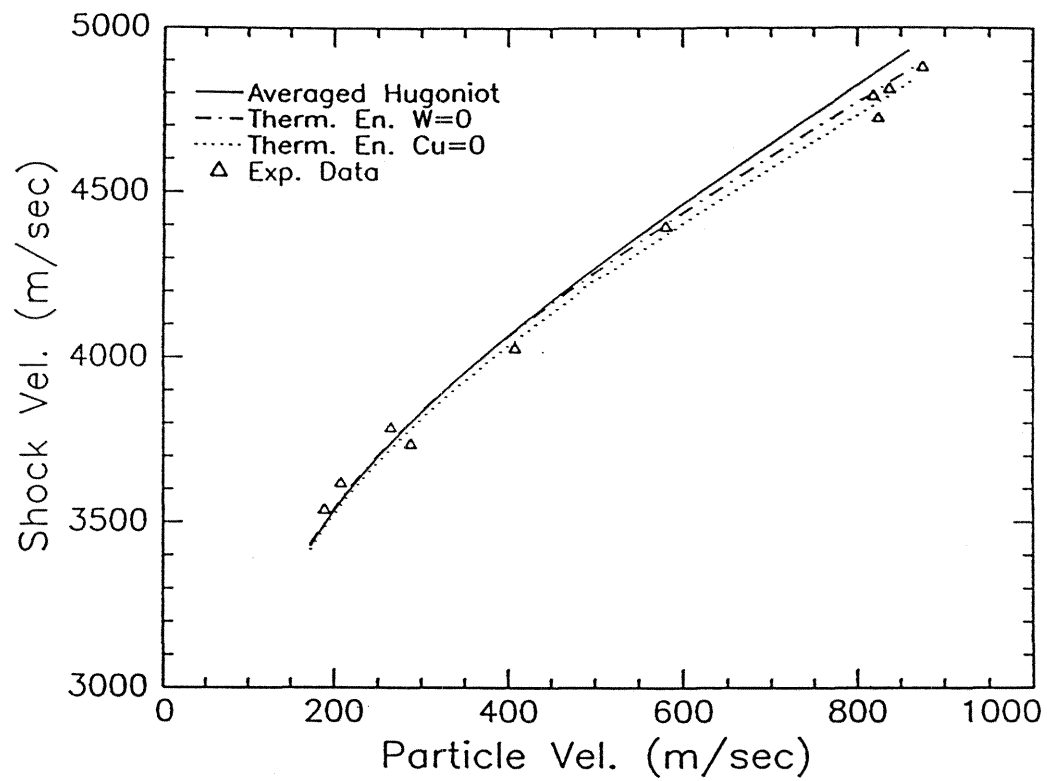


FIG. 2. Calculated and experimental Hugoniot of sintered W infiltrated with 24 wt.% Cu. The distension calculated from the experimental data is 1.014.

### 3. SHOCK INITIATION OF THE REACTION FORMING NiSi

#### 3.1 Shock Initiated Chemical Reactions in 1:1 Atomic Percent Nickel–Silicon Powder Mixtures

B.R. Krueger, T. Vreeland, Jr.

W. M. Keck Laboratory of Engineering Materials

California Institute of Technology, 138–78

Pasadena, CA 91125

#### ABSTRACT

A series of shock initiated chemical reaction experiments have been performed on 1:1 atomic percent mixtures of nickel and silicon powders. It has been observed that only minor surface reactions occur between the constituents until a thermal energy threshold is reached above which the reaction goes to completion as evidenced by large voids, bulk melting, and scanning electron microscopy and x-ray diffraction results. The experiments show the energy difference between virtually no and full reaction is on the order of 5 percent. A sharp energy threshold indicates that with the particular morphology used, the bulk temperature determines whether or not the reaction occurs rather than local, particle level, conditions.

#### INTRODUCTION

The first systematic investigation of the shock-induced formation of intermetallic compounds was reported by Horie et al.[1,2,3] Aluminides of Ni and Ti were formed from mechanically mixed elemental powders. More recently, Song and Thadhani presented further studies on the shock synthesis of Ni aluminides.[4] These investigators concluded that shock-enhanced reactivity strongly influenced

the synthesis process.

A series of experiments have been performed on two mixtures of 1:1 atomic percent elemental nickel and silicon powders in a well characterized propellant driven plate system. The experiments reveal the existence of a thermal energy threshold below which little or no reactions occur and above which full reaction occurs as evidence by bulk melting and x-ray diffraction and scanning electron microscopy (SEM) results. The experiments also show the width of the threshold to be on the order of 5 percent. From the existence of a sharp thermal energy threshold, certain conclusions can be made about the parameters which determine whether or not bulk reactions occur.

## EXPERIMENT

Two mixtures of 1:1 atomic percent (67.6 wt % Ni) powders of Ni and Si were used. The first, Mix A, consisted of 15  $\mu\text{m}$  spherical Ni from Inco Metals and -325 mesh irregular Si of unknown purity. The second, Mix B, was 20  $\mu\text{m}$  - 45  $\mu\text{m}$  spherical nickel (Aesar Stock # 10581) and -325 mesh irregular silicon (Cerac Stock # S-1052). The elemental powders were mechanically mixed in petroleum ether to avoid particle agglomeration and then dried. No special care was taken to remove or prevent formation of oxides on the particle surfaces. Optical images of the two mixtures are shown in Figures 1a and 1b.

The shock facility used is the Keck Dynamic Compactor, a 35 mm smooth bore cannon. Experiments with a metallic glass have shown that the gun and target assemblies used result in highly one dimensional shock conditions.[5] A 5 mm 303 stainless steel plate was used as the flyer. The geometry of the target assembly limits the shock duration by the reflection from the back of the flyer plate, and therefore the duration is governed by the flyer thickness. The effects of duration have not been explored. The shock facilities are discussed in further detail in Ref. 1.

Preliminary experiments were conducted with porous bronze inserts, pressed into a target fixture, which contain 4 smaller cavities. These experiments have the advantage of identical impact conditions for each sample and four samples per shot. A disadvantage is that the impedance mismatch between the inserts and samples may give rise to two dimensional effects. To insure that two dimensional effects were not the determining factor, critical results were confirmed using a full cavity.

## RESULTS AND ANALYSIS

The shock conditions were determined using an averaging method which assumes that the mixture's bulk modulus is linear with pressure and the mixture's Grüneisen parameter to specific volume ratio is constant. With these assumptions, the Rankine-Hugoniot relationships and the known Hugoniot of the flyer, the mass averaged shock conditions can be determined.[6] The homogeneous shock temperature was determined by matching the thermal energy to the integration of the mixture's heat capacity of the form  $C = a + 10^{-3}bT + 10^5c/T^2$ , where  $C$  is the heat capacity and  $T$  is temperature. No attempt was made to correct the heat capacity for pressure effects. The thermodynamic parameters used are listed in Table I, and the calculated shock results of the experiments discussed below are listed in Table II.

The first set of experiments were conducted with Mix A. The green's porosity was typically 40%, and flyer velocities were varied from 700 to 1600 m/sec. Optical microscopy of the compacts recovered from low energy shots showed no evidence of chemical reactions, and the compacts were poorly bonded. In higher energy shots, the reaction apparently went to completion as evidenced by large voids, bulk melting and a homogeneous appearance under the optical microscope.

Further experiments showed the energy difference between no and full reaction to be small. In a four cavity experiment at a flyer velocity of 1.02 km/sec,

no reactions occurred in a sample pressed to a porosity of  $35.9 \pm 0.8$  percent while the reaction went to completion in the sample pressed to a porosity of  $41.1 \pm 0.8$  percent. These porosities and impact conditions correspond to calculated homogeneous temperatures of  $594^\circ \text{C}$  and  $622^\circ \text{C}$ , respectively, or a total energy difference of less than 4 percent. Two full cavity experiments confirmed the energy difference to be less than 12 percent. No attempt was made using full cavities to narrow down the threshold width further.

An analogous procedure was conducted with Mix B. Since the morphologies of the two mixtures are similar, it is not surprising that the results for Mix B are nearly identical. A four cavity experiment showed the energy threshold to lie between thermal energies corresponding to homogeneous temperatures of  $631^\circ \text{C}$  and  $648^\circ \text{C}$ , or a total energy difference of less than 3 percent. Full cavity experiments confirmed that the separation in total energy between no and full reaction was less than 10 percent. No attempt was made using full cavities to narrow down the threshold width further. It is interesting to note that, except for the very small amount of surface reactions discussed below, no compacts of either mixture were recovered in an intermediate condition between no and full reaction.

Scanning electron microscopy of compacts shocked to just below the reaction threshold revealed that minor surface reactions had occurred which are not detectable optically or with x-ray diffraction. As can be seen in the back scattered electron image shown in Figure 3, the extent of the reaction was very limited. The nature of the reacted region differed slightly between Mix A and Mix B. The reactions in Mix A were very uniform along the interfaces where they occurred with a typical thickness of  $0.5 \mu\text{m}$ . The Mix B compact also had a uniform reaction zone on a small portion of the interfaces, but there also existed pools of reacted material. A back scattered electron image of a typical reacted interface for mix B is shown in Figure 4, which also contains the far more typical interface showing no reaction.

## DISCUSSION

From the existence of a sharp threshold, it can be reasoned that the shock parameter governing whether or not bulk reactions occur in a 1:1 mixture of this particular morphology is the homogeneous temperature. The experiments rule out the possibility that the threshold is a pressure or elastic energy effect since the more porous compacts react but are shocked to a lower pressure and elastic energy.

One may argue that local particle level conditions change significantly across the threshold, however any such explanation is unlikely since it must exclude the possibility that the same local conditions exist anywhere at lower shock energies. For example, the existence/kinetics of shock initiated chemical reactions has been explained by local mass mixing and other similar terms describing local differences in the particle velocities of the constituents.[7-9] However, as can be seen in Figure 2, there is no evidence of mass mixing, and it is unlikely that increasing the energy by as little as 3 percent will greatly enhance mass mixing, especially with a lower shock pressure since one would expect greater constituent mixing at greater pressures.

Another local condition which may arguably change as the threshold is crossed is that a critical melt pool size is attained, however this is also not likely. Since the energy difference between practically no and full reaction is small, there is a high probability that there exists some local pre-shock particle configuration in the less porous green which will result in a "critical" melt pool size upon compaction. Furthermore, if the reaction is determined by some local pre-shock particle configuration, reactions would occur sporadically, depending on local particle placement during the pressing of the greens. Another argument may be that a critical density of melt pools is attained above the threshold, however this can not be true since, in the time it takes to "communicate" between melt pools through heat conduction, the melt pools no longer exist.[10] It is possible to argue

other particle level explanations, however, as mentioned above, a necessary feature of such an approach would be that the same local conditions can not exist in lower energy samples.

We therefore conclude that the homogeneous temperature determines whether or not reactions occur in 1:1 atomic percent Ni/Si mixtures of the particular morphologies used here. This is the only parameter which undoubtedly varies across threshold and is a reasonable explanation as to why lower energy compacts do not react while slightly higher energy compacts react fully. Since the homogeneous temperature determines whether or not bulk reactions occur, one can also conclude that the reaction kinetics are slower than the time required for temperature equilibration. Assuming a linear heat conduction time constant of,  $\tau = r^2/\kappa$ , where  $r$  is the Ni particle radius and  $\kappa$  is nickel's thermal diffusivity, gives that the reaction occurs on a time scale greater than several microseconds.[10]

## CONCLUSION

Experiments on two mixtures of similar morphology of 1:1 atomic percent Ni and Si powders reveal the existence of a sharp energy threshold below which no significant reactions occur and above which the reaction goes to completion as evidenced by bulk melting and SEM and x-ray diffraction results. From the existence of a sharp energy threshold, it can be reasoned that the homogeneous temperature determines whether or not the bulk reaction occurs rather than particle level conditions. One can also conclude that the reaction occurs on a time scale greater than several microseconds.

## ACKNOWLEDGEMENTS

This work was supported under the National Science Foundation's Materials Processing Initiative Program, Grant No. DMR 8713258. We would like to thank

Phil Dixon, formally at the New Mexico Institute of Technology for preparing Mix B.

#### REFERENCES

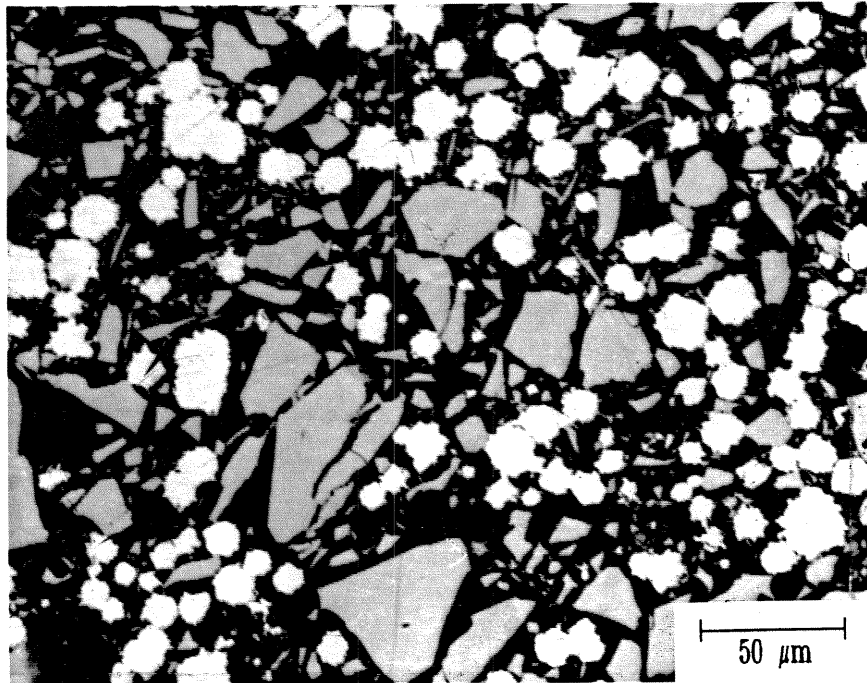
- [1] Y. Horie, R. A. Graham and I. K. Simonsen, *Mat. Lett.* **3**, 354 (1985).
- [2] Y. Horie, R. A. Graham and I. K. Simonsen, in "Metallurgical Applications of Shock-Wave and High-Strain-Rate Phenomena," L. E. Murr, K. P. Staudhammer, and M. A. Meyers (eds.), Marcel Dekker, New York, 1023 (1986).
- [3] N. N. Thadhani, M. J. Costello, I. Song, S. Work, and R. A. Graham, in "Solid-State Powder Processing," A. H. Clauer and J. J. deBarbadillo (eds.), The Minerals, Metals, and Materials Society, Warrendale, PA, 97 (1990).
- [4] I. Song and N. N. Thadhani, presented at the TMS Symposium on Reaction Synthesis of Materials, New Orleans, (Feb. 1991), to be published in *Met. Trans.*
- [5] A. H. Mutz and T. Vreeland, Jr., in "Shock Waves and High-Strain-Rate Phenomena in Materials," M. A. Meyers, L. E. Murr, and K. P. Staudhammer (eds), Marcel Dekker, Inc., New York, (1991, in Press).
- [6] The averaging method used was similar to M. B. Boslough, *J. Chem. Phys.* **92**, 1839 (1990).
- [7] S. Batsanov et al., *Combustion, Explosions and Shock Waves* **22**, 65 (1986). 65.
- [8] R. A. Graham et al. in "Shock Waves in Condensed Matter," Y. M. Gupta (ed.), Plenum Press, New York, 693 (1986).
- [9] M. B. Boslough and R. A. Graham, *Chem. Phys. Lett.* **121**, 446, (1985).
- [10] R. B. Schwarz, P. Kasiraj and T. Vreeland, Jr., in "Metallurgical Applications of Shock Waves and High-Strain-Rate Phenomena," L. E. Murr, M. A. Meyers and K. P. Staudhammer (eds.), Marcel Dekker, New York, 313 (1986).

Table I. Thermodynamic parameters used to determine the Hugoniot of the Ni/Si mixtures. The isentropic bulk modulus of Ni and the Grüneisen parameters for Ni and Si were taken or calculated from V.N. Zharkov and V.A. Kalinin, Equations of State for Solids at High Pressures and Temperatures, Consultants Bureau, New York, 1971. The pressure derivative of the isentropic bulk modulus of Ni was determined by fitting solid Ni Hugoniot data. Silicon's isentropic bulk modulus and its pressure derivative were taken from O.L. Anderson, J. Phys. Chem. Solids 27, 547 (1966). The heat capacity coefficients were taken from, E.A. Brandes (ed.), Smithells Metal Reference Book, Sixth Edition, Butterworth & Co., 8-42 (1983). The units of a, b and c are J/(mole-K), J/(mole-K<sup>2</sup>) and J-K/mole, respectively.

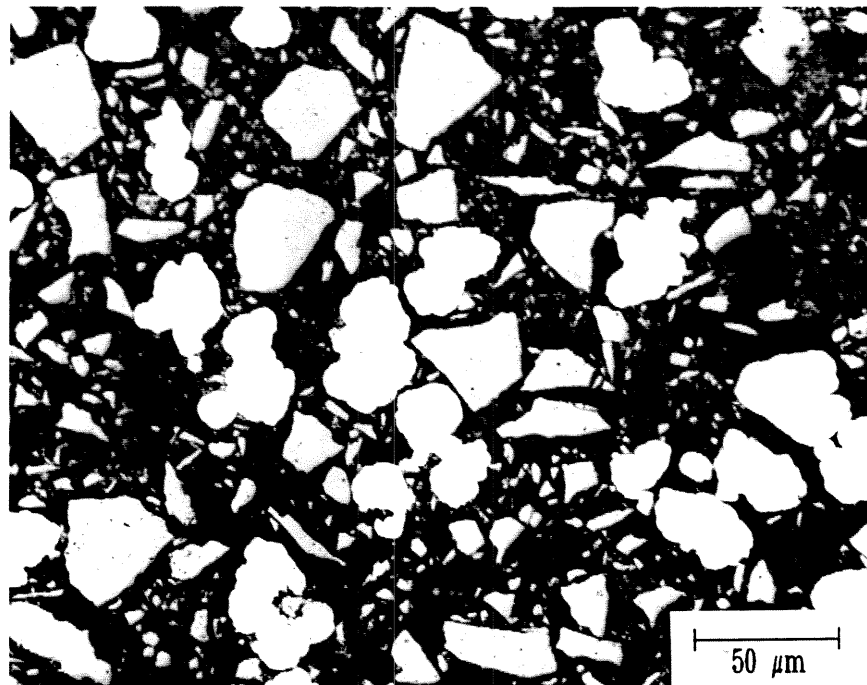
Density (g/cm <sup>3</sup> )	$\beta_s$ (GPa)	$\left. \frac{\partial \beta_s}{\partial P} \right _s$	$\gamma_0$	a	b	c
Ni( $\alpha$ ) 8.90	192.5	3.94	1.91	17.00	29.48	0
Ni( $\beta$ ) 8.90	192.5	3.94	1.91	25.12	7.54	0
Si 2.33	97.9	4.19	0.74	23.95	2.47	-4.14

Table II. The calculated shock conditions of the experiments discussed in the text. The column headings correspond to the mixture, porosity, flyer velocity, pressure, total energy, thermal energy, homogeneous temperature (assuming no reaction), and whether or not the reaction occurred, respectively. An asterisk indicates a four cavity experiment. The enthalpy of formation of NiSi at 298° K is  $-43.1$  kJ/mole or  $-593$  kJ/kg from W. Oelsen, H. O. von Samson–Himmelstjerna, Mitt. K.–W.–I. Eidenforsch., Dusseldorf, 18, 131 (1936). The ratio of energy input from the shock plus the energy generated by the reaction to the energy needed to heat and melt NiSi is 1.23 for the lowest shock energy which triggered the reaction.

Mix	Por. (%)	Vel. (m/sec)	P (GPa)	E (kJ/kg)	$E_T$ (kJ/kg)	$T_{Hnr}$ (°C)	React. (Y/N)
A	37.5	1000	5.37	364	352	581	N
A	42.8	1040	4.95	413	404	660	Y
A*	35.9	1020	5.87	374	359	594	N
A*	39.7	1020	5.21	389	378	622	Y
B	37.5	1020	5.60	380	367	605	N
B	41.2	1060	5.38	421	410	670	Y
B*	37.5	1050	5.86	398	384	631	N
B*	39.9	1050	5.46	407	396	648	Y



(a) Mix A



(b) Mix B

FIG. 1 Optical images of the Ni + Si mixes. The lighter particles are Ni.

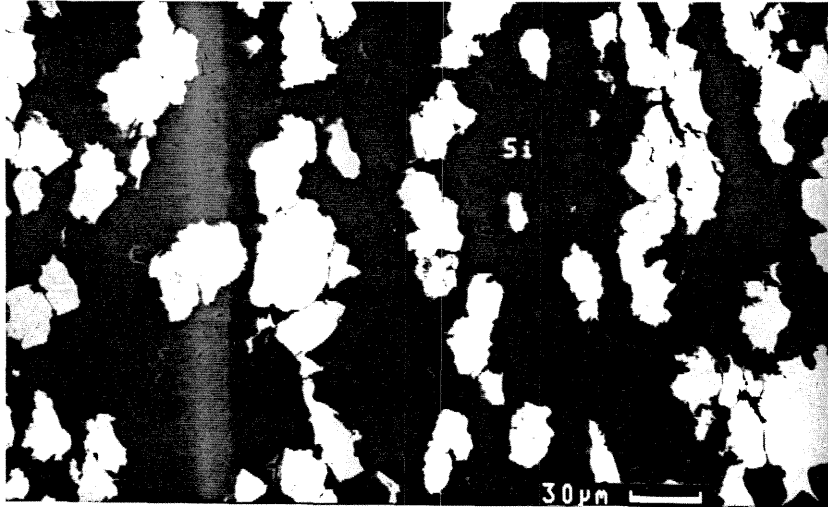


FIG. 2 SEM back scattered image of Mix B shocked in a full cavity experiment to an energy just below where bulk reaction occurs. At this magnification, there is little evidence of any interaction between the Ni and Si. The shock propagated from right to left.

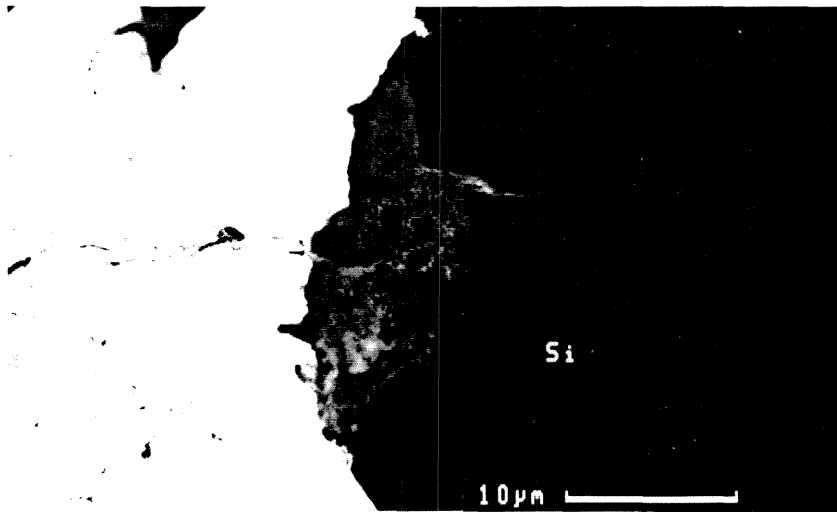


FIG. 3 SEM back scattered image of Mix B shocked in a full cavity experiment to an energy just below where bulk reaction occurs. At this magnification, small interfacial reactions can be seen as well as pools of reacted material. Also shown are interfaces where no reactions are detectable, by far the large majority.

### 3.2 Correlation of Shock Initiated and Thermally Initiated Chemical Reactions in a 1:1 Atomic Ratio Nickel–Silicon Mixture

Barry R. Krueger, Andrew H. Mutz, and Thad Vreeland, Jr.

W. M. Keck Laboratory of Engineering Materials

California Institute of Technology, 138–78

Pasadena, CA 91125

#### ABSTRACT

Shock initiated chemical reaction experiments have been performed on a 1:1 atomic ratio mixture of 20  $\mu\text{m}$  to 45  $\mu\text{m}$  nickel and –325 mesh crystalline silicon powders. It has been observed that no detectable or only minor surface reactions occur between the constituents until a thermal energy threshold is reached, above which the reaction goes to completion. The experiments show the energy difference between virtually no and full reaction is on the order of 5 percent. The level of the thermal energy threshold is found to correspond to the temperature at which statically pressed powders begin to react in a differential thermal analyzer (DTA). A sharp energy threshold and a direct correlation with DTA results indicates that, with the the particular powder morphologies used, the homogeneous shock temperature determines whether or not the reaction occurs rather than local, particle level conditions. From this it may be concluded that the reaction occurs on a time scale greater than the time constant for thermal diffusion into the particle interiors.

## INTRODUCTION

Shock initiated chemical reactions are currently of considerable interest.[1-6] With the high pressure and temperature associated with shock wave processing, it may be possible to concurrently synthesize and form near net shape parts of intermetallic compounds and other materials. Shock processing is also a viable technology for producing composite materials where it is necessary to control chemical reactions between the matrix and reinforcing particle since such reactions often have deleterious effects on the mechanical properties of the composite.

The chemistry and kinetics of intermetallic reactions have been explored by observing the behavior of multilayer thin films upon heating. It has been shown that in many multilayer composite structures, self-sustaining chemical reactions can be initiated upon heating.[7-11] Bordeaux, Yavari, and Desre[8] place two basic criteria on whether or not such reactions are possible. Briefly, the first is that the heat of the reaction must be in excess of that required to melt the mixture, and the second is that the rate of heat generation due to the reaction must be greater than the rate of heat dissipation to the environment. Thermally initiated reactions which are not self-sustaining have been observed in Ni/Si multilayers as well as in a number of other metallic multilayers. The temperature at the onset of the reaction is observed to increase somewhat with the heating rate.[11] Ma et al.[12] observed an "explosive" reaction propagating at about 4 m/s in thin multilayers of Ni/Al and observed a layer thickness effect. Reactions did not propagate when the layer thickness exceeded a critical value, and they suggested that the critical layer thickness is proportional to the ratio of the heat released by the reaction to the heat dissipated to the environment, which increases with ambient temperature.

Olowolafe et al.[13] observed the growth of nickel silicide layers upon heating Ni films vacuum deposited on a single crystal, polycrystalline, and amorphous Si (a-Si) annealed from 200° C to 325° C. Only Ni<sub>2</sub>Si formed on (111) and (100) Si

and on polycrystalline Si while  $\text{Ni}_2\text{Si}$  and NiSi formed in two distinct sublayers on a-Si. Ma et al.[14] observed solid state interdiffusion reactions in Ni film and a-Si bilayers, and observed only crystalline  $\text{Ni}_2\text{Si}$  formation with high purity a-Si. For the case where the a-Si contained about 5% carbon an amorphous  $\text{Ni}_2\text{Si}$  layer was also observed. Clevenger and Thompson,[15] using isothermal and constant heating rate differential thermal analysis (DTA) of evaporated multilayer films of Ni and a-Si (2 Ni to 1 Si), found distinct exothermic peaks associated with the formation of amorphous nickel silicide and crystalline  $\text{Ni}_2\text{Si}$ .

Combustion synthesis (CS or SHS, self-propagating high temperature synthesis) of intermetallic and other systems employs a thermally initiated self-sustaining chemical reaction. In CS, the reaction is externally initiated in one section of a usually porous sample, with a specific contact area between particles much less than in multilayer films. The sample may be in either a vacuum or at atmospheric pressure. The reaction then propagates through the sample at a rate lower than that observed in the explosive reaction of multilayers, driven by the heat of reaction conducting and radiating into the unreacted material.[13]

The initiation of reactions by shock waves in chemically active powder mixtures is similar to thermal initiation in that the shock wave deposits a significant amount of thermal energy in the sample. The thermal energy is deposited through the plastic deformation associated with void collapse and relative inter-particle motion, however the shock wave also produces conditions which have no counterpart in thermally initiated reactions. From a macroscopic point of view, the shock process is different in that the material in the shock front is very rapidly heated (with heating rates in excess of  $10^{10}$  K/s) and raised to a pressure of typically several GPa for a duration on the order of microseconds, and the material behind the shock attains particle velocities on the order of hundreds of meters per second. SHS reactions typically propagate at velocities of less than 1 m/s.

A shock wave which triggers a reaction typically travels at a velocity on the order of 1 km/s. Therefore substantial reaction may not occur in the shock front unless the powder particles are of sub-micron size, but the reaction will be initiated throughout the powder on a time scale much shorter than in the usual SHS reaction.

On the particle level, the shock process is also quite different from thermally initiated reaction. As a shock wave passes through a porous media, energy is deposited preferentially near the particle exteriors.[17] In ductile powders the particle exterior are deformed significantly more than the interiors in the closing of voids. The preferential deposition of shock energy results in a positive temperature gradient from interior to the exterior of the particle. The time required for temperature equilibration is dependent upon the thermal properties of the materials, particle size, and melt pool size (when the shock energy is sufficient to cause melt to form). The homogeneous shock temperature is defined as the temperature of the shocked compact after local particle thermal equilibrium has been achieved, and before the compact conducts significant heat to the surrounding ambient. Assuming spherical particles, spherically homogeneous energy deposition and no melt pools, Schwarz et al.[18] gave the time constant for temperature equilibration to be  $r^2/16D$ , where  $r$  is the particle radius, and  $D$  is the thermal diffusivity of the powder. Temperature measurements in shocked powders of Cu and constantan confirmed this relationship and excellent agreement between the measured homogeneous temperature and the homogeneous temperature calculated from the shock energy was demonstrated.[19]

Graham et al.,[20] Thadhani et al.,[21] Batsanov et al.,[22] and others have reported studies on shock initiated chemical reactions in a number of systems. They have put forth several qualitative reasons for why the shock initiated chemical reaction process might be very different from the other synthesis processes described above. These reasons are summarized in what Graham has coined "catastrophic

shock" as opposed to "benign shock." Benign shock, as discussed by Horie et al.,[23] is a description of the shock process from the traditional viewpoint of the macroscopic conservation equations, with void collapse and the resulting inhomogeneous energy deposition and the normal processes of thermal equilibration and atomic diffusion. The catastrophic shock concept views the interaction of shock waves with chemically reactive media through the formation of activated complexes, non-diffusive transport of matter described as relative mass motion and fluid-like flow, and the critical involvement of crystal defects in chemical reactions.

We have recently reported the results of a series of shock initiated reaction experiments on two similar mixtures of 1:1 atomic ratio elemental nickel and silicon powders.[24] These experiments were conducted using a propellant gun and target design which results in highly one-dimensional shock conditions, and therefore, in uniform shock conditions over the majority of the sample. It was found that there exists a thermal energy threshold below which only minor surface reactions occur and above which the reaction goes to completion as evidenced by spherical voids in the recovered compacts indicative of bulk melting. These experiments show the threshold is crossed with an energy increase on the order of 5 percent. It was argued that the narrowness of the threshold indicates that the homogeneous temperature rather than the pressure effects and local inhomogeneities determine the initiation of the reaction forming NiSi. The current work provides further evidence that the homogeneous temperature is the critical parameter determining whether or not bulk reactions occur and that phenomena described as "catastrophic" shock may be of secondary importance in this chemical system.

## EXPERIMENT

The mixture of 1:1 atomic ratio (67.6 wt % Ni) elemental Ni and Si consisted of 20  $\mu\text{m}$  - 45  $\mu\text{m}$  nickel (Aesar Stock # 10581) and -325 mesh crystalline silicon

(Cerac Stock # S-1052). The powders were mechanically mixed in petroleum ether to avoid particle agglomeration and then dried. No special care was taken to remove or prevent the formation of oxides on the particle surfaces. A back-scattered SEM micrograph of the starting mixture is shown in Figure 1.

The shock facility used is the Keck Dynamic Compactor which employs a 35 mm smooth bore launch tube. In our target, the flyer plate strikes the sample directly and does not strike the sample containment fixture, a schematic of which is shown in Figure 2. There exists strong evidence that the target assembly and impact conditions result in highly one-dimensional, and therefore well defined, shock conditions as discussed below.

Figure 3 shows metallic glass ( $\text{Ni}_{76.4}\text{Cr}_{19.7}\text{B}_{2.3}\text{C}_{0.08}$ ) which has been shock consolidated with a 5 mm thick 304 stainless steel flyer at a velocity of 1 km/sec.[25] The sample has been cut with a low speed diamond saw, polished and etched with Marbles reagent. The shock propagated from left to right in the figure. A macro-photograph of the recovered compact is inset to the right of the figure, and an optical micrograph of the region of changing contrast is on the left. X-ray diffraction has confirmed that the darkened region crystallized while the light region remained amorphous, Although the properties of this metallic glass are not well characterized, the transition region occurs at a distance from the flyer/sample interface at which a release wave from the rear of the flyer is expected to overtake the initial shock. This strongly implies that the shock energy heated the compact to a temperature in excess of the crystallization temperature. The sample's salient feature is the highly planar interface between the two uniform regions indicating nearly one-dimensional shock conditions.

Although a numerical simulation has not been conducted for our target fixture, a recently presented simulation of a similar target indicates that the target assembly and impact conditions used should result in highly one-dimensional shock

conditions.[23] For the simulation, a thick cover plate was assumed, and to achieve one-dimensional conditions, it was determined that the ratio of the flyer to sample diameters should be slightly greater than one. With our target and impact conditions, no cover plate is used and the flyer to sample diameter ratio is equal to one. Although the precise effect of these differences has not been investigated, the similarity in the two target designs indicates that deviations from one-dimensional shock conditions should be small.

Finally, a simple argument shows that shock parameters calculated assuming one-dimensional conditions give the maximum pressure and shock energy in the sample, given that the release wave from the rear of the flyer overtakes the initial shock within the powder sample (the thickness of the powder sample was adjusted to assure this in the present investigation). Since the sample containment fixture is not impacted, the pressure at the sample edges releases radially in the target and containment fixture, and there is no increase of pressure due to the "wrap-around" waves which occur when the sample as well as the target fixture is impacted by the flyer.[27-29]

In all the experiments, a 5 mm thick 303 stainless steel plate was used as the flyer. Flyer velocities were measured by timing the interruption of two light beams just prior to impact. A doppler radar system was used to verify that the flyer achieves a nearly constant terminal velocity before it reaches the light beams. As discussed above, the geometry of the target assembly limits the maximum shock duration in the powder by the reflection from the back of the flyer plate, and therefore the maximum shock duration is governed by the material and thickness of the flyer and the shock wave velocity in the powder. The effects of shock duration were not explored in this investigation. The launch tube and target were evacuated to about 0.1 torr prior to impact.

Preliminary shock experiments were conducted with porous bronze inserts,

with four separate powder cavities, pressed into a target fixture (Figure 4).[30] These experiments have the advantage of identical impact conditions for each of four samples per shot. A disadvantage is some impedance mismatch between the insert and samples due to a difference in porous and solid density and wave speed between the samples and porous bronze. This impedance mismatch will give rise to some two-dimensional effects. To check that the two-dimensional effects were not governing the reaction initiation in the four cavity experiments, critical experiments were repeated using targets filled with only the powder mixture. The results of full and four cavity experiments presented below were in good agreement.

The differential thermal analysis experiments were performed on a DSC 2000 manufactured by Setaram Corporation, France. DTA samples were pressed in a simple cylinder and die assembly made of C350 maraging steel to allow static pressures as high as approximately 1.5 GPa.

## RESULTS

The shock conditions were determined using an averaging method which assumes the shock pressure and particle velocity of the two constituents are equal; the mixture's bulk modulus is linear with pressure, and the mixture's Grüneisen parameter to specific volume ratio is constant. With these assumptions, the Rankine-Hugoniot relationships and the known Hugoniot of the flyer, the mass averaged shock conditions can be determined. The properties were averaged according to the following formulas:

$$V_{0AB} = \sum_i x_i V_i, \quad (1)$$

$$\left[ \frac{V}{\gamma} \right]_{0AB} = \sum_i x_i \left[ \frac{V}{\gamma} \right]_{0i}, \quad (2)$$

$$\beta_{0SAB} = V_{0AB} \left[ \sum_i \frac{x_i V_{0i}}{\beta_{0Si}} \right]^{-1}, \quad (3)$$

$$\beta'_{0SAB} = \left[ \frac{\beta_{0SAB}^2}{V_{0AB}} \sum_i x_i V_{0i} \left[ \frac{1 + \beta'_{0Si}}{\beta_{0Si}^2} \right] \right] - 1. \quad (4)$$

The subscript AB refers to the mixture. The subscript i refers to the individual components. The subscript 0 refers to standard conditions, and  $V$ ,  $\gamma$ ,  $\beta_{0S}$ ,  $\beta'_{0S}$  are the specific volume, Grüneisen parameter, isentropic bulk modulus, and the pressure derivative of the isentropic bulk modulus at constant entropy, respectively.

The homogeneous shock temperatures were determined by matching the calculated thermal energies to an integration of the mixture's heat capacity of the form  $C = a + 10^{-3}bT + 10^5c/T^2$ , where  $C$  is the heat capacity and  $T$  is temperature.[33] No attempt was made to correct the heat capacity for pressure effects. The thermodynamic parameters used are listed in Table I, and the impact conditions and calculated shock parameters of the experiments discussed below are listed in Table II.

A four cavity shock experiment was then performed where the initial porosity of the samples and flyer velocity (Table II) were chosen to give homogeneous temperatures either just below or just above the reaction onset temperature found in preliminary experiments. It should be noted that with a given flyer velocity, the shock energy *increases* with powder porosity while the shock pressure and the shock and particle velocities *decrease* with porosity. The two lower energy compacts recovered showed no evidence of chemical reactions with either optical or x-ray diffraction analysis, and the compacts were poorly bonded. In the two higher energy samples, the reaction apparently went to completion as evidenced

by large spherical voids indicative of bulk melting and a homogeneous appearance under the optical microscope. The threshold was found to lie between thermal energies of 384 and 396 J/g, corresponding to homogeneous temperatures of 631° C and 648° C, or a total energy difference of less than 3 percent. Full cavity experiments confirmed the energy threshold to be at the same level and that the separation in total energy between no and full reaction was less than 10 percent. No attempt was made using full cavities to further narrow the threshold width.

X-ray diffractions scans of the Ni/Si powder mixture shocked to just below and just above the energy threshold were made. Only Ni and Si diffraction peaks were observed in the samples shocked to just below the threshold, and optical as well as SEM examination of polished sections revealed a porosity less than 1%. All diffraction peaks observed in the sample shocked to just above the threshold were indexed as orthorhombic NiSi indicating that the reaction goes to completion once the energy threshold is crossed. It is important to note that in these experiments no compacts were recovered in an intermediate condition between no and full reaction.

DTA experiments were performed on statically pressed powders. It was found that the onset temperature of the first significant exothermic reaction was dependent upon the porosity of the DTA samples. Four DTA scans on statically pressed powder are shown in Figure 5 corresponding to 50% porosity (tap density), a porosity of 32%, a porosity of 27%, and a porosity of 23%. As can be seen, the onset temperature increases with increasing porosity. The magnetic transformation at 360° C is seen on all of the scans.

A DTA run of the mixture shocked to an energy just below the threshold where the reaction occurs is also plotted in Figure 5. It can be seen that the onset of the reaction occurs at a temperature 30° C below that found in powder statically compressed to 23% porosity. Apparently, the unreacted powders were not significantly modified by the shock process except that the porosity was reduced.

Scanning electron microscopy of a full cavity compact shocked to just below the reaction threshold revealed that isolated mixing had occurred which was not detected optically or with x-ray diffraction. The mixing occurred in regions which appear to have been shock-induced melt pools. As can be seen in the back-scattered electron image shown in Figure 6, the extent of the mixing was very limited. A higher magnification back-scattered electron image of a mixed region is shown in Figure 7, which was found to be 21% Ni and 79% Si by dispersive x-ray analysis.

## DISCUSSION

Clemens et al.[34] observed an energy threshold for the formation of an amorphous alloy from layered nickel-zirconium films which were heated by microsecond current pulses. The sudden onset of reaction at the threshold energy was attributed to chemical energy of the reaction, and the change in diffusion kinetics as the sample temperature exceeded the glass transition temperature of the amorphous alloy. We postulate that in the shocked Ni-Si powder the chemical energy and the shock energy cause the sample temperature to exceed the NiSi melting temperature at the threshold shock energy.

Bordeaux et al.[8] observed a small increase in reaction temperature with an increase in DTA heating rate in Pd-Sn and Zr-Al reactions triggered by melting of one component of the mixture. The small increase in reaction temperature with heating rate observed for Ni-Si mixtures (going from 621° C at 10° C/min for shock compacted but unreacted powder to about 640° C at about  $10^{10}$  ° C/s for shock reacted powder) is comparable to that observed by Bordeaux et al.[8] in Pd-Sn and Zr-Al for a 60-fold rate increase.

The rapid temperature rise in the shock prevents build-up of diffusion barriers by solid state reactions which can occur at typical DTA scan rates. The

mixing reaction time is thereby decreased without significantly changing the time for dissipation of the heat of reaction to the environment. This leads to a self-sustaining reaction in the shocked mixture when the heat of mixing is sufficiently large as Bordeaux et al.[8] have postulated. Static pressing brings more particle surface area into contact and also tends to break-up oxide layers which leads to lowered onset temperatures for the reaction.

From the existence of a sharp threshold and the correlation of the homogeneous shock temperature corresponding to the thermal energy threshold level at the onset temperature of the reaction in the DTA, it can be reasoned that the shock parameter governing whether or not bulk reactions occur in a 1:1 mixture of this particular morphology is the homogeneous shock temperature. The experiments rule out the possibility that the threshold is a pressure or elastic energy effect since the more porous compacts react but are shocked to a lower pressure and elastic energy.

One may argue that local particle level conditions change significantly across the threshold, however any such explanation is suspect since it must exclude the possibility that the same local conditions exist anywhere at lower shock energies. For example, the occurrence of shock initiated chemical reactions has been explained by local mass mixing due to local differences in the particle velocities of the constituents.[22] However, as can be seen in Figures 6 and 7, there is no evidence of mass mixing outside of melt pools and thin isolated surface layers, and it is unlikely that increasing the energy by as little as 3 percent will greatly enhance mass mixing, especially combined with a lower shock pressure and particle velocity, as one would expect less constituent mixing as these shock parameters decrease.

Another local condition which may arguably change as the threshold is crossed is that a critical melt pool size is attained, however this is also not likely. Since the energy difference between practically no and full reaction is small, there is

a high probability that there exists some local pre-shock particle configuration in the less porous green which will result in a "critical" melt pool size upon compaction. Another argument may be that a critical density of melt pools is attained above the threshold, however this cannot be true since, in the time it takes to "communicate" between melt pools through heat conduction, the melt pools no longer exist. It is possible to argue other particle level explanations, but a necessary feature of such an approach would be that the same local conditions cannot exist in samples shocked to slightly lower energy.

The experimental findings and the above arguments are fully consistent with recent work on self-sustained reactions in metal-metal multilayer composites by Bordeaux, Yavari, and Desre,[8] and their description of these reactions is analogous to what we believe is occurring in the Ni/Si mixtures used here.

We therefore conclude that the homogeneous temperature determines whether or not reactions occur in 1:1 atomic ratio Ni/Si mixtures of the particular morphologies used here. Since the homogeneous temperature determines whether or not bulk reactions occur, one can also conclude that the reaction kinetics are slower than kinetics of temperature equilibration in the particles. Therefore, the reaction proceeds on a time scale greater than several microseconds when the particle size exceeds about 10 microns.

## CONCLUSION

Experiments on mixtures of 1:1 atomic ratio Ni and Si powders reveal the existence of a sharp energy threshold below which no significant reactions occur and above which the reaction goes to completion as evidenced by SEM and x-ray diffraction results and voids indicative of bulk melting. The level of the thermal energy threshold corresponds to the onset temperature of the reaction in statically compressed powders in a DTA scan. From the existence of a sharp energy threshold

and the correlation to DTA results, it can be reasoned that the homogeneous shock temperature determines whether or not the bulk reaction occurs rather than particle level conditions. These results are consistent with experiments in multilayer metal-metal composites, and we believe the phenomenological criteria put forth by Bordeaux et al.[8] for these reactions adequately explains the basic nature of the shock reaction process in the Ni/Si mixtures and morphologies used here. One can also conclude that the reaction occurs on a time scale greater than several microseconds.

#### ACKNOWLEDGEMENTS

This work was supported under the National Science Foundation's Materials Processing Initiative Program, Grant No. DMR 8713258. We would like to thank Phil Dixon, formally at the New Mexico Institute of Technology, for preparing the powder mixture, and Zezhong Fu of Caltech for her help with the DTA experiments.

#### REFERENCES

- [1] S. S. Batsanov, S. Doronin, S. V. Klochdov, and A. I. Teut in "Combustion, Explosions and Shock Waves," 22, 765 (1986).
- [2] R. A. Graham, B. Morison, Y. Horie, E. L. Venturini, M. B. Boslough, M. Carr, and D. L. Williamson, in "Shock Waves in Condensed Matter," Y. M. Gupta (ed.), Plenum Press, New York, 693 (1986).
- [3] N. N. Thadhani, M. J. Costello, I. Song, S. Work, and R. A. Graham, in "Proceedings of the TMS Symposia on Solid State Powder Processing," Indianapolis, to be published (October 1-4, 1989).
- [4] N. N. Thadhani, A. Advani, I. Song, E. Dunbar, A. Grebe, and R. A. Graham, in "Proceedings of the International Conference on High Strain-rate Phenomena in Materials," UCSD (August 1990) Explomet '90 (in press, 1991).

- [5] M. B. Boslough, *J. Chem. Phys.* 92, 1839 (1990).
- [6] L. H. Yu and M. A. Myers, *IBID.*
- [7] L. A. Clevenger, C. V. Thompson, and R. C. Cammarata, *Appl. Phys. Lett.* 52, 795 (1988).
- [8] F. Bordeaux, A. R. Yavari, and P. Desre, *Rev. Phys. Appl.* 22, 707 (1987).
- [9] J. A. Floro, *J. Vac. Sci. Technol.* A4, 631 (1986).
- [10] F. Bordeaux, Doctoral Thesis, Institut National Polytechnique de Grenoble, (October 1989).
- [11] F. Bordeaux and A. R. Yavari, *J. Mater. Res.* 5, 1656 (1990).
- [12] E. Ma, C. V. Thompson, L. A. Clevenger, and K. N. Tu, *Appl. Phys. Lett.* 57, 1262 (1990).
- [13] J. O. Olowolafe, M-A. Nicolet, and J. W. Meyer, *Thin Solid Films* 38, 143 (1976).
- [14] E. Ma, W. J. Meng, W. L. Johnson, and M-A. Nicolet, *Appl. Phys. Lett.* 53, 2033 (1988).
- [15] L. A. Clevenger and C. V. Thompson, *J. Appl. Phys.* 67, 1325 (1990).
- [16] J. B. Holt, *Mater. Res. Bull.* 12, 60 (1987).
- [17] W. H. Gourdin, *Prog. Mater. Sci.* 30, 39 (1986).
- [18] R. B. Schwarz, P. Kasiraj, T. Vreeland, Jr. and T. J. Ahrens, *Acta Metall.* 32, 1243 (1984).
- [19] R. B. Schwarz, P. Kasiraj, and T. Vreeland, Jr. in "Metallurgical Applications of Shock-Wave and High-Strain-Rate Phenomena," L. E. Murr, K. P. Staudhammer, and M. A. Myers (eds.), Marcel Dekker, New York, 331 (1986).
- [20] R. A. Graham, B. Morosin, Y. Horie, E. L. Venturini, M. B. Boslough, M. Carr, and D. L. Williamson, in "Shock Waves in Condensed Matter," Y. M. Gupta (ed.), Plenum Press, New York, 693 (1986).

- [21] N. N. Thadhani, M. J. Costello, I. Song, S. Work, and R. A. Graham, in "Solid State Powder Processing," A. H. Clauer and J. J. DeBarbadillo (eds.), Minerals, Metals and Materials Society, Warrendale, PA (1990).
- [22] S. S. Batsanov, G. S. Doronin, S. V. Klochdov, and A. I. Teut, "Combustion, Explosions and Shock Waves" 22, 765 (1987).
- [23] Y. Horie and M. E. Kipp, J. Appl. Phys. 63, 5718 (1988).
- [24] B. R. Krueger and T. Vreeland, Jr., in "Shock Waves and High-Strain-Rate Effects in Materials", M. A. Myers, L. E. Murr, and K. P. Staudhammer (eds.), Marcel Dekker, New York (1990, in press).
- [25] J. Bach, B. Fultz, and B. R. Krueger, research in progress.
- [26] T. Thomas, P. Bensussan, P. Chartagnac, and Y. Bienvenu, see Reference #4.
- [27] R. A. Graham and D. M. Webb, in "Shock Waves in Condensed Matter," J. R. Asay, R. A. Graham, and G. K. Straub (eds.), Elsevier, 211 (1984).
- [28] G. E. Korth, J. E. Flinn, and R. C. Green, see Reference #19, 129.
- [29] T. Akashi and A. B. Sawaoka, U. S. Patent No. 4 658 830 (April 7, 1987).
- [30] A. H. Mutz and T. Vreeland, Jr., see Reference #26.
- [31] V. N. Zharkov and V. A. Kalinin, in "Equations of State for Solids at High Pressures and Temperatures," Consultants Bureau, New York (1971).
- [32] O. L. Anderson, J. Phys. Chem. Solids 27, 547 (1966).
- [33] "Smithells Metal Reference Book, 6th edition," E. A. Brandes (ed.), Butterworth and Co., 8-42 (1983).
- [34] B. M. Clemens, R. M. Gilenbach, and S. Bitwell, Appl. Phys. Lett. 50, 495 (1987).

Table I. Thermodynamic parameters used to determine the Hugonoids of the Ni/Si mixtures. The isentropic bulk modulus of Ni and the Grüneisen parameters for Ni and Si were taken or calculated from Reference 31. The pressure derivative of the isentropic bulk modulus of Ni was determined by fitting solid Ni Hugoniot data. Silicon's isentropic bulk modulus and its pressure derivative were taken from Reference 32. The heat capacity coefficients were taken from Reference 33. The units of a, b, and c are J/(mole-°K), J/(mole-°K<sup>2</sup>), and J-°K/mole, respectively.

Density (g/cm <sup>3</sup> )	$\beta_s$ (GPa)	$\left. \frac{\partial \beta_s}{\partial P} \right _s$	$\gamma_0$	a	b	c
Ni( $\alpha$ ) 8.90	192.5	3.94	1.91	17.00	29.48	0
Ni( $\beta$ ) 8.90	192.5	3.94	1.91	25.12	7.54	0
Si 2.33	97.9	4.19	0.74	23.95	2.47	-4.14

Table II. The calculated shock conditions of the experiments discussed in the text. The column headings correspond to the mixture, porosity, flyer velocity, pressure, total energy, thermal energy, homogeneous temperature (assuming no reaction), and whether or not the reaction occurred, respectively. An asterisk indicates a four cavity experiment. The enthalpy of formation of NiSi at 298° K is  $-43.1$  kJ/mole or  $-593$  J/g from W. Oelsen, H. O. von Samson-Himmelstjerna, Mitt. K.-W.-I. Eidenforsch., Düsseldorf 18, 131, (1936). The ratio of energy input from the shock plus the energy generated by the reaction to the energy needed to heat and melt NiSi is 1.23 for the lowest shock energy which triggered the reaction.

Porosity (%)	Velocity (m/s)	P (GPa)	E (J/g)	$E_T$ (J/g)	$T_{Hnr}$ (°C)	React. (Y/N)
37.5	1020	5.60	380	367	605	N
41.2	1060	5.38	421	410	670	Y
37.5*	1050	5.86	398	384	631	N
39.9*	1050	5.46	407	396	648	Y

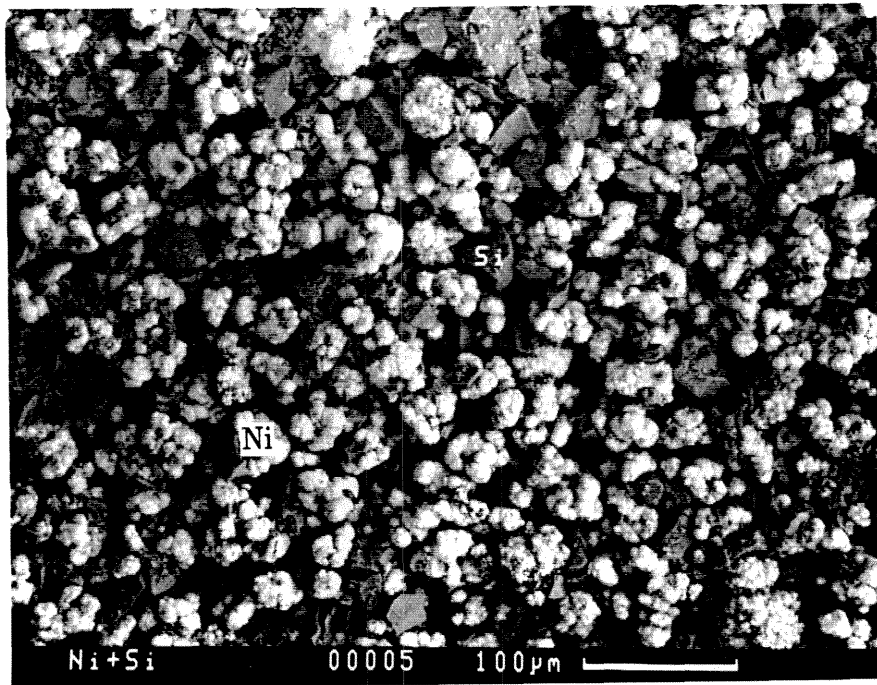


Figure 1. Back-scattered SEM micrograph of the Ni/Si powder mixture showing the morphology of the lumpy spherical Ni and the irregular Si.

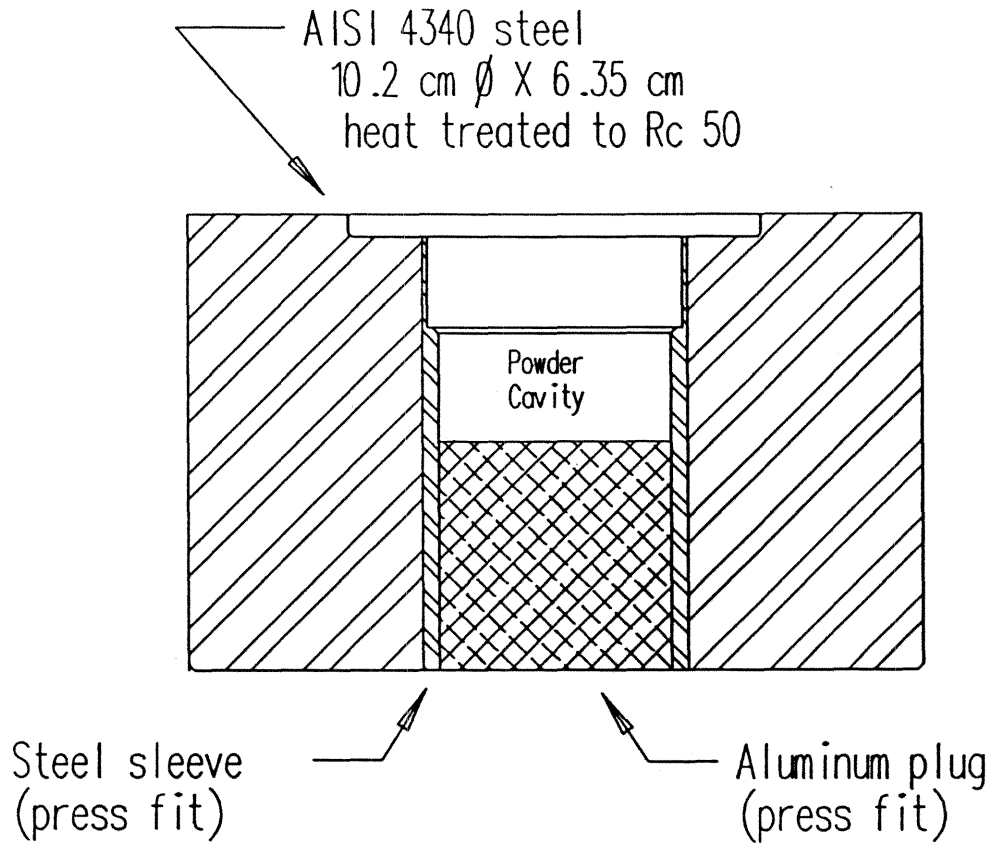


Figure 2. Schematic drawing of the target design. The top surface is "O" ring sealed to the barrel and the bottom surface is pressed against a momentum trap.

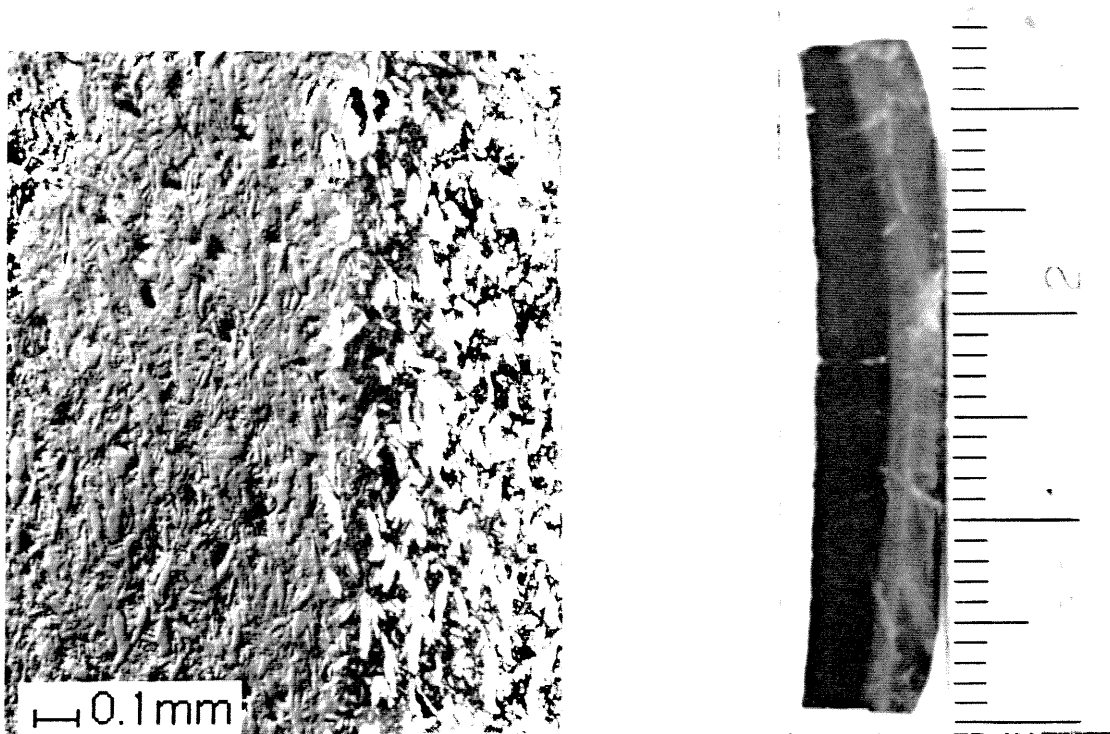


Figure 3. Optical micrograph of a shock consolidated metallic glass powder (left), with a macro-photograph of the sectioned compact (right). The shock wave propagated from left to right, and the region on the left of the compact is crystalline. Note the planar shape of the transition region between the crystalline phase (darker phase) and the glass phase (non-etching) which is located at the position where the release wave from the back of the flyer caught the shock wave.

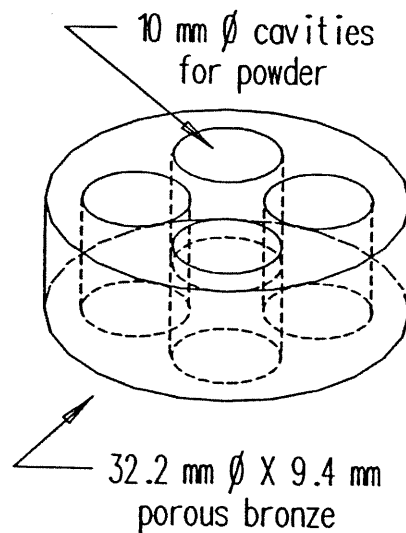


Figure 4. Porous bronze insert machined with four cavities for powder samples.

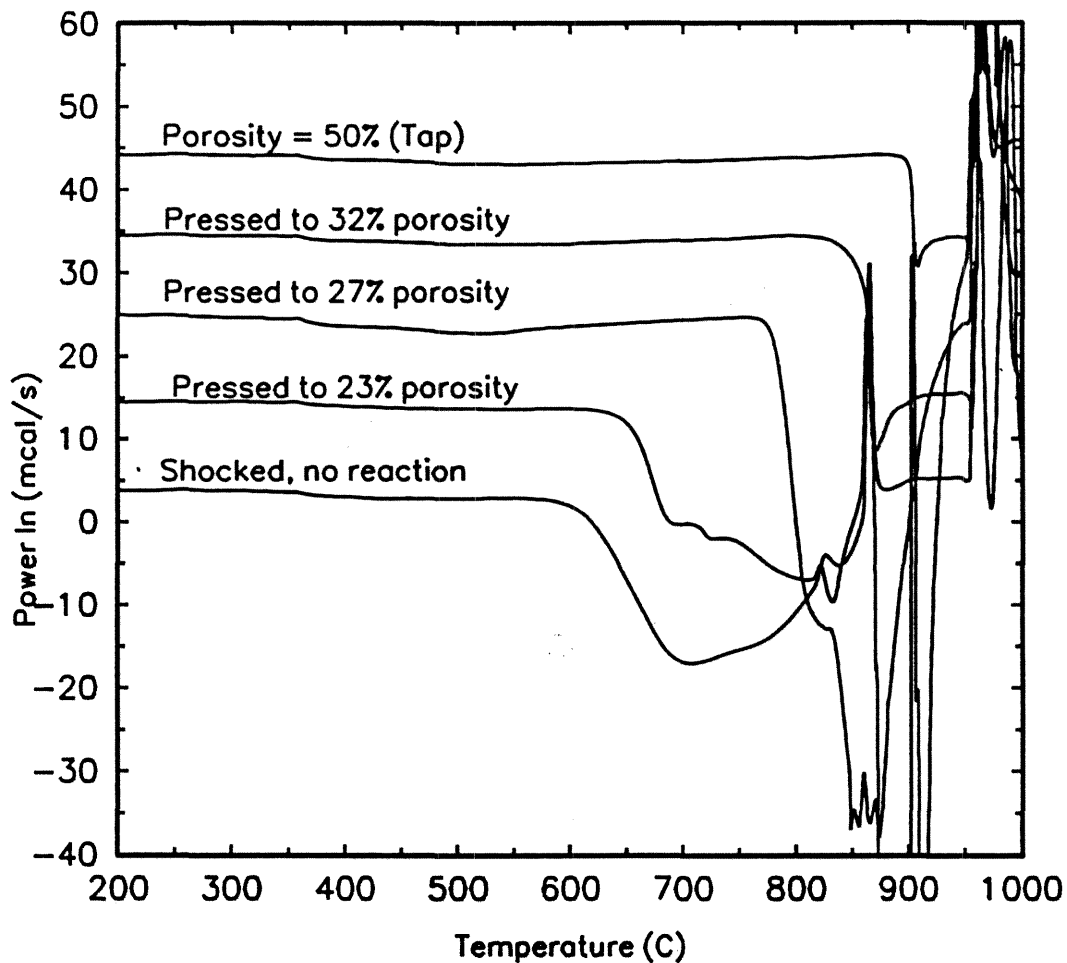


Figure 5. DTA scans of Ni/Si powder statically pressed to four different porosities and a shock compressed but unreacted powder (porosity near zero). Note that the onset temperature of the exothermic reaction increases with porosity. Heating rate was  $10^{\circ}$  K/min, and scans are successively displaced by 10 mcal/s from the scan below.

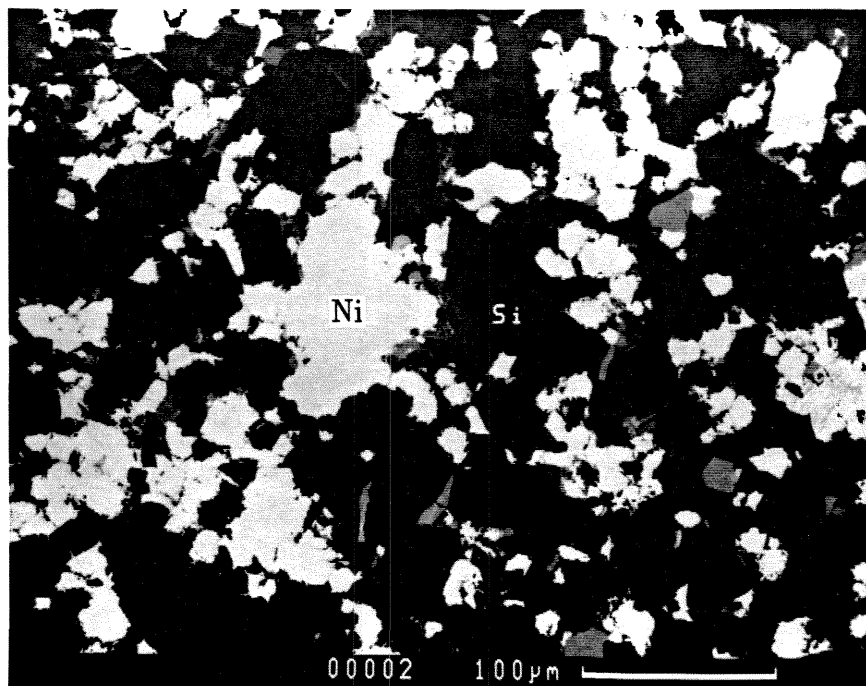


Figure 6. SEM back scattered image of the Ni/Si powder mixture shocked in a full cavity experiment to an energy just below where bulk reaction occurs. At this magnification, there is little evidence of any interaction between the Ni and Si.

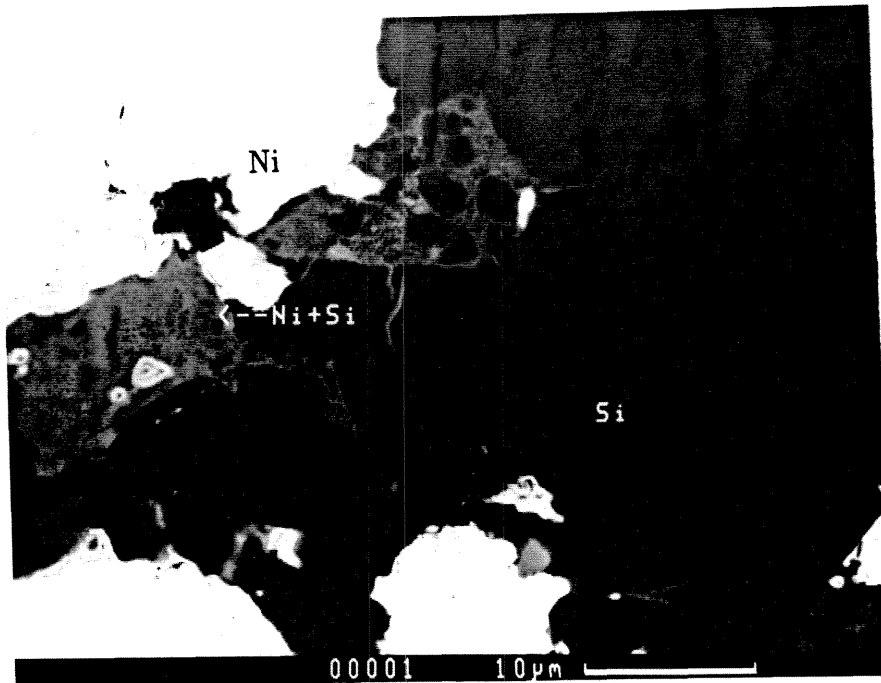


Figure 7. SEM back-scattered image of the Ni/Si powder mixture shocked in a full cavity experiment to an energy just below where bulk reaction occurs. At this magnification, some small interfacial mixed regions are observed as well as isolated pools of a mixture of Ni and Si. The more typical interfaces show no mixing.

## 4. SHOCK INITIATION OF THE REACTION FORMING $Ti_5Si_3$

### 4.1 Shock Induced Reactions in 5:3 Atomic Ratio Titanium/Crystalline Silicon Powder Mixtures

B. R. Krueger, A. H. Mutz and T. Vreeland, Jr.

W. M. Keck Laboratory of Engineering Materials  
California Institute of Technology, Pasadena, CA 91125

#### ABSTRACT

The conditions for initiation and propagation of the reaction forming  $Ti_5Si_3$  from elemental powders of varying porosity have been investigated using shock waves of different pressure in vacuum, and using hot wire ignition in an argon atmosphere. In each case the reaction either went to completion, or the powder remained essentially unreacted. The conditions for the propagation of the reaction depend upon the presence of residual air as well as the initial porosity and the shock pressure. Two regimes of porosity and pressure are found for the Ti/Si mixture which cause complete reaction. A low energy regime with a high initial porosity (producing a low shock pressure) with residual air triggers the reaction while no reaction is observed with a 128% higher shock energy and a lower initial porosity (producing a higher shock pressure) when the residual air is replaced with argon. Hot wire ignition of porous powder at room temperature initiates a self-propagating high temperature synthesis reaction (SHS) more easily in air than in an argon atmosphere, while the Ni/Si powder must be heated to allow the SHS reaction to propagate in high or low porosity mixtures in air. These observations are compared to published work on self-sustaining reactions in multilayer films.

## INTRODUCTION

A recently completed study of shock-initiated reactions in equiatomic Ni/Si powder found a threshold shock energy for the reaction forming NiSi.[1] The threshold was determined to be between 384 and 396 J/g, corresponding to homogeneous temperatures of 631 and 648° C in the consolidated mixture. The current study explores the shock conditions for the reaction forming  $Ti_5Si_3$  from an elemental mixture of the powders.

The chemistry and kinetics of intermetallic reactions have been explored by observing the behavior of multilayer elemental thin film composites upon heating. It has been shown that in many composite structures, self-sustaining chemical reactions can be initiated upon heating. Bordeaux and Yavari place two basic criteria on whether or not such reactions are possible.[2] Briefly, the first is that the heat of the reaction must be sufficiently in excess of that required to melt the mixture, and the second is that the mixing reaction time must be much shorter than the time for dissipation of the heat of reaction to the environment. Thermally initiated reactions which are not self sustaining have been observed in Ti/Si multilayers as well as in a number of other metallic multilayers. Differential thermal analysis (DSC) of Ni/Si powders pressed or shocked to low porosity show exothermic reactions starting in the temperature range of the homogeneous shock temperature for initiation of the reaction.[3] Solid state interdiffusion studies of Ni as well as Ti layers on high purity amorphous and crystalline Si show the metal silicide phase forms upon deposition and extends upon annealing, with the compound phases forming as equilibrium is approached.[4] The DSC scans show at least two exothermic peaks, the first due to the amorphous silicide formation and the second due to crystallization of the silicide.

SHS reactions in elemental powder mixtures have been extensively explored at atmospheric pressure. They may be initiated at one end of a porous sample and

may propagate in a homogeneous or heterogeneous mode. Analytic expressions describing the propagation of SHS reactions have been developed.[5,6] Relevant parameters are the rate of heat release in the reaction front, and the rate of heat loss by thermal conduction and radiation. Reaction fronts typically propagate at velocities less than 1 m/s. A shock wave which triggers a reaction typically travels at a velocity on the order of 1 km/s in a powder mixture and reduces the porosity and deposits shock energy in powder particles in times on the order of 10 ns (for particles of about 20  $\mu\text{m}$  diameter). Therefore substantial reaction may not occur in the shock front unless the powder particles are of sub-micron size, but the reaction will be initiated throughout the powder on a time scale much shorter than in the usual SHS reactions.

The initiation of SHS reactions at atmospheric pressure in Ni/Si and Ti/Si powder mixtures was compared in the present study. These observations suggest possible explanations for the different initiation conditions found for reactions in shocked Ni/Si and Ti/Si powder mixtures.

## EXPERIMENT

Aesar -325 mesh Ti powder (99.5% nominal purity) was wet mixed in 1,1,2-trichloro-1,2,2-trifluoroethane with Cerac -325 mesh crystalline Si powder (99.5% nominal purity) in a 5:3 atomic ratio and dried in vacuum. Figure 1a is a SEM image of the powder mixture, and Figure 1b is a SEM image of the Ni/Si powder mixture, which has Ni particles more spherical than the Ti but with the same Cerac Si.

Shock experiments were conducted on powders using propellant driven stainless steel flyer plates and a target which produces well controlled plane-wave shock geometry.[3] The barrel and powder mixture were evacuated to 0.1 Torr just prior to each experiment. In one set of experiments the powder was evacuated from

atmosphere. The remainder were backfilled with argon and then evacuated. Table I lists the results of these experiments on powders pressed to different initial porosity. Shock pressures and energies for the powder mixture were calculated using averaged properties for an inert elemental mixture.[1] The calculation of homogeneous temperatures from the shock energy used heat capacities which were not corrected for pressure and did not include reaction energies.

The shocked samples were examined by x-ray diffraction, and only  $\text{Ti}_5\text{Si}_3$  diffraction peaks were observed in the reacted samples. Only Ti and Si peaks were observed in the unreacted samples. An optical micrograph of a polished surface of the recovered sample shocked to 0.8 GPa and mounted in plastic is shown in Figure 2. The highly porous sponge-like structure is typical of SHS material which melted at atmospheric pressure or in vacuum with the evolution of gases.[7] Figure 3 is a back-scattered SEM image of the unreacted shock consolidated Ti/Si mixture shocked to 2.29 GPa. The Si particles show extensive fracture and no evidence of local mixing or melting. Ni/Si powder shocked to just below the reaction threshold is shown in the back-scattered SEM image of Figure 4. The Si particles have fractured, and isolated regions of a mixture of Ni and Si are observed in what appear to have been melt pools. The mixed region in Figure 4 was found to be 21 atomic % Ni and 79 atomic % Si by EDX.

The SHS ignition behavior of both equiatomic ratio Ni/Si powders and 5:3 atomic ratio Ti/Si powders of high porosity (about 55%) and low porosity (near zero, shock consolidated but unreacted) was observed. A 0.13 mm Ta wire was placed in contact with the sample and a voltage which brought the wire to a white heat was applied to the ends of the wire. The powders were tested in air as well as in Ar to minimize oxidation. The low porosity powders did not ignite. The high porosity Ti/Si ignited more readily in air than in Ar, and the high porosity Ni/Si did not react. A SHS reaction in high porosity Ti/Si in contact with low porosity

Ti/Si resulted in complete reaction. The low porosity Ni/Si was not ignited by contact with a SHS reaction in high porosity Ti/Si.

## DISCUSSION

The shock initiated reaction in the Ti/Si mixture shows a more complex energy dependence than the Ni/Si mixture. The Ti/Si mixture exhibits reaction behavior which depends upon shock energy, initial porosity (or shock pressure), and residual gas. A shock energy of 104 J/g initiated the reaction to  $\text{Ti}_5\text{Si}_3$  with residual air, while no reaction was observed at a shock energy of 237 J/g with residual Ar. The reaction occurs with a combination of low porosity and low shock pressure with residual air which gives low shock energy, or with high shock energy with residual air or Ar. The heat of reaction for the formation of NiSi is 85.8 kJ/mole (42.9 kJ/g-atom to solid at 25° C) while that for the formation of  $\text{Ti}_5\text{Si}_3$  is 580 kJ/mole (72.5 kJ/g-atom). The critical conditions for the self-sustaining reaction according to Bordeaux et al. [2] are: a) the heat of mixing must be sufficiently in excess of the energy to melt the mixture, and b) the mixing reaction time must be much shorter than the time required for dissipation of the heat of reaction to the surrounding material to prevent quenching of the reaction. The critical condition a) is met in both systems when the minimum shock energy observed for reaction initiation is added to the reaction energy. Thermal conductivities of Ni, Ti, and Si at ambient conditions are 0.91, 0.22, and 1.49 W/(cm-° K) respectively. The rate of heat dissipation is greater in the Ni/Si system and the reaction energy is smaller. Both conditions a) and b) favor SHS reactions in the Ti/Si mixture as observed in this investigation. The strong effect of residual air on both shock and SHS initiation may be explained by the exothermic reaction caused by the oxidation of Ti. The sponge-like structure of the shock reacted material indicates the presence of a liquid phase after the shock pressure was

removed (after approximately 1  $\mu$ s). Powder treatment to remove surface contaminants such as titanium hydrides should significantly reduce the porosity of the recovered titanium silicide.

## CONCLUSIONS

1. The shock-induced reaction forming  $Ti_5Si_3$  from the stoichiometric elemental powder mixture of Ti and Si exhibits a dependence on shock energy, initial porosity, and residual oxygen.
2. SHS reactions are more readily initiated in the Ti/Si mixture than in equiatomic Ni/Si powder mixtures with comparable particle sizes.
3. High shock and chemical reaction energies and low thermal conductivity appear to favor self-propagating reactions in shocked powders as proposed by Bordeaux et al. for thin film elemental composites.[2]
4. The reaction produces a sponge-like structure, indicating that the reaction initiated by the shock formed solid  $Ti_5Si_3$  at atmospheric pressure.

## ACKNOWLEDGEMENTS

This work was supported under the National Science Foundation's Materials Processing Initiative Program, Grant No. DMR 8713258. Barry Krueger died on October 29, 1990 as a result of injuries received in a motorcycle accident. His family, friends, and scientific colleagues mourn the loss of a truly gifted individual.

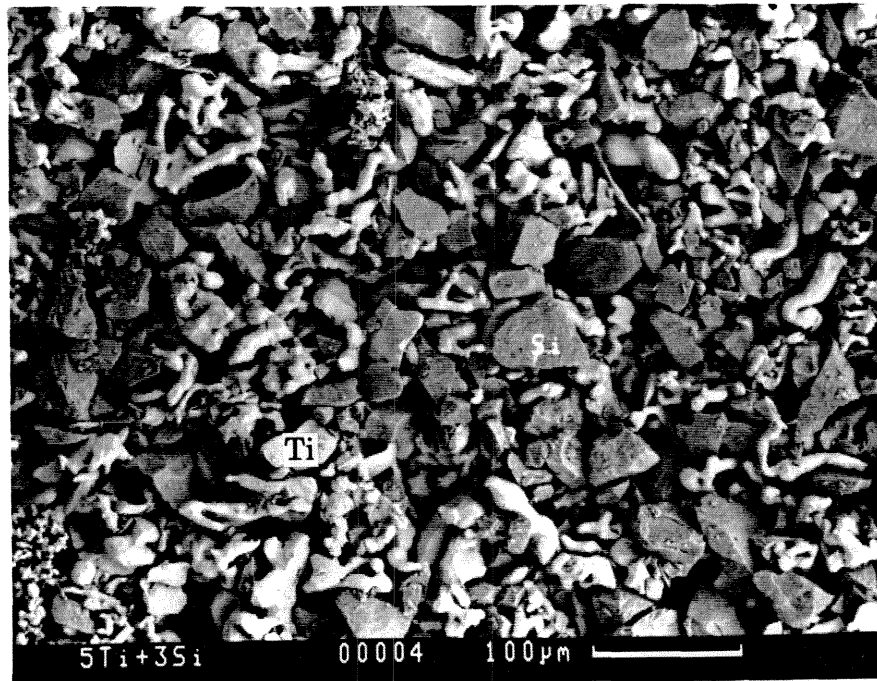
## REFERENCES

- [1] B. R. Krueger and T. Vreeland, Jr., in "Shock Waves and High-Strain-Rate Effects in Materials," M. A. Meyers, L. E. Murr, and K. P. Staudhammer (eds.), Marcel Dekker, New York, (1991, in press).
- [2] F. Bordeaux and A. R. Yavari, *J. Mater. Res.* 5, 1656 (1990).
- [3] B. R. Krueger, A. H. Mutz, and T. Vreeland, Jr., source cited in Reference #1.
- [4] K. Holloway and R. Sinclair, *J. Appl. Phys.* 61, 1359 (1987).
- [5] A. A. Zenin, A. G. Merzhanov, and G. A. Nersisyan, *Combust. Explos. Shock Waves (Engl. Trans.)* 17, 63 (1981).
- [6] T. Boddington, P. G. Laye, J. Tipping, and D. Whalley, *Combust. Flame* 63, 359 (1986).
- [7] W. F. Henshaw, A. Niiler, and T. Leete, ARBRL-MR-03354. Ballistics Research Laboratory, Aberdeen Proving Ground, MD, 1984.

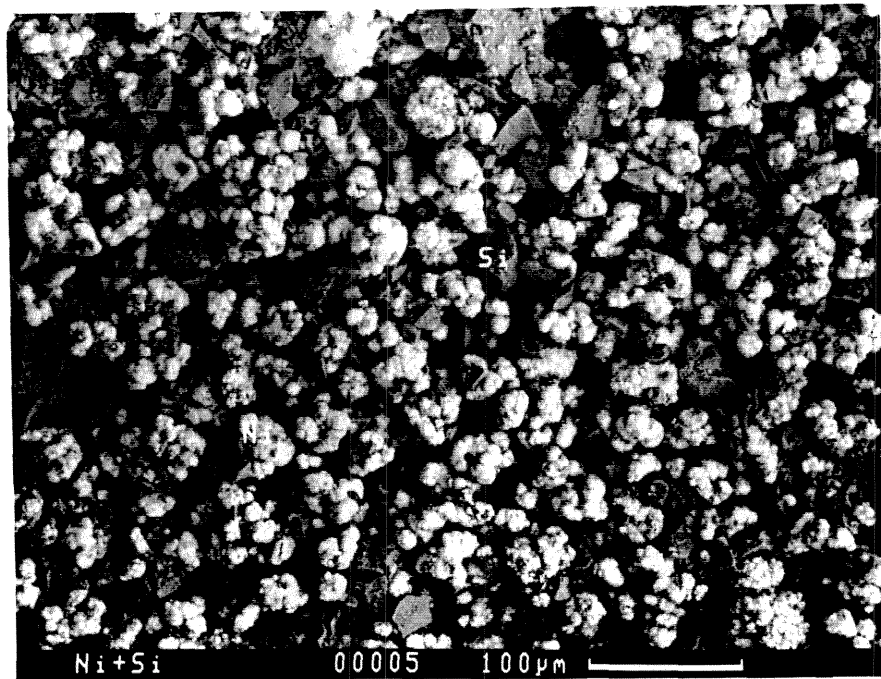
Table I. Shock Reaction Experiments

Flyer Velocity (m/s)	Porosity (%)	Shock Energy (J/g)	Homogeneous Temperature (°C)	Shock Pressure (GPa)	Reaction
480	48.7	104	192	0.80	Yes
487	49.2	108	198	0.8	No †
514	47.4	118	214	0.95	Yes
570	48.7	145	256	1.11	Yes
575	44.4	144	254	1.31	No
693	46.0	206	349	1.76	No †
757	42.9	237	396	2.29	No †
837	44.4	293	470	2.61	Yes †
915	48.7	350	560	2.67	Yes †
965	48.7	386	610	2.95	Yes †

† Powder backfilled with argon and evacuated before shock treatment



(a)



(b)

Figure 1. Back-scattered SEM micrograph of (a) the Ti/Si powder mixture, and (b) the Ni/Si powder mixture.

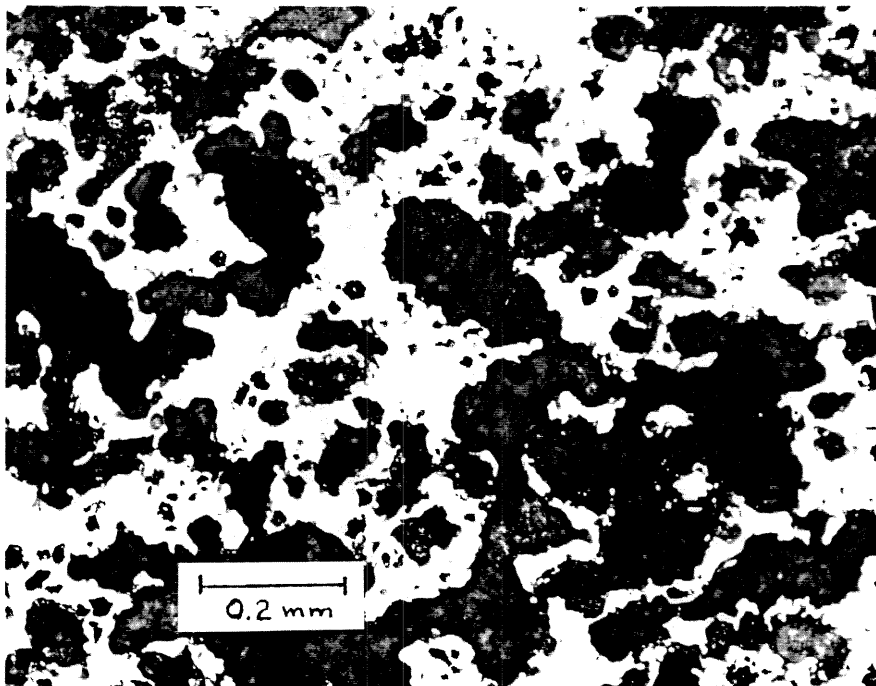


Figure 2. Optical micrograph of the recovered Ti/Si powder mixture which was shocked to 0.8 GPa showing a sponge-like structure identified as  $\text{Ti}_5\text{Si}_3$  by x-ray diffraction.

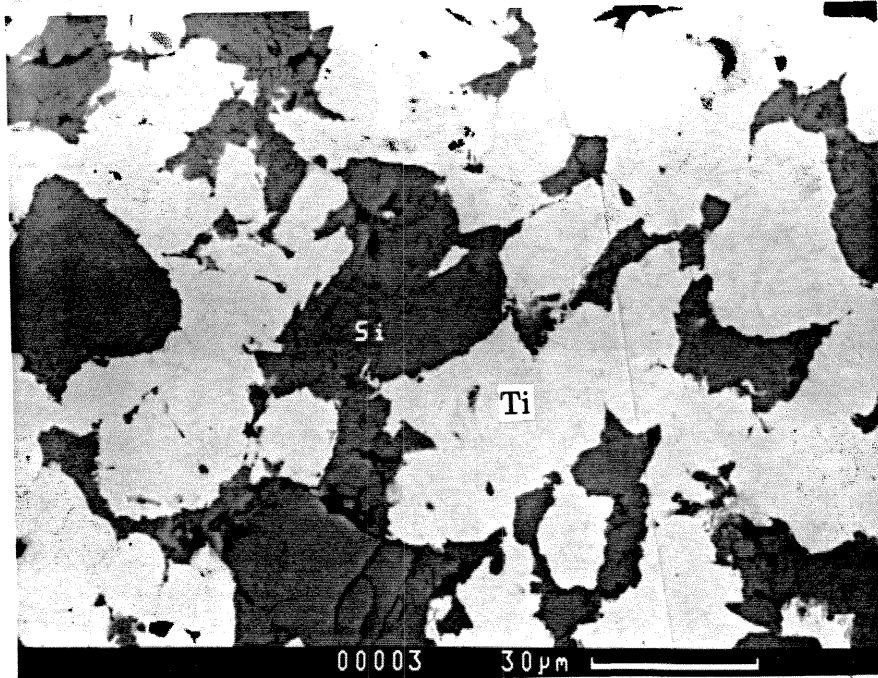


Figure 3. Back-scattered SEM micrograph of unreacted Ti/Si shocked to 2.29 GPa. No titanium silicides were found in x-ray diffraction or EDX analyses.

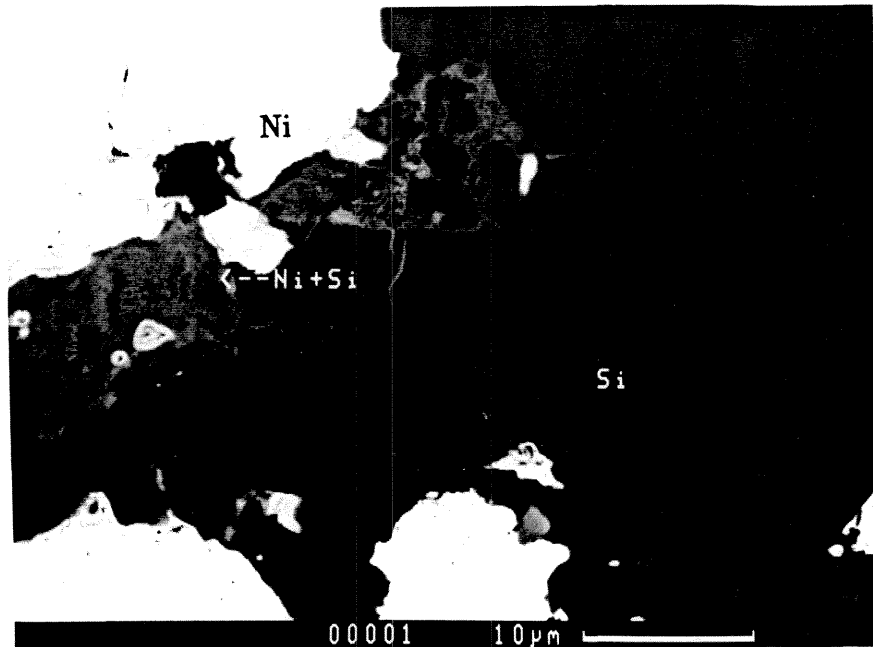


Figure 4. Back-scattered SEM micrograph of a Ni/Si powder mixture (1:1 atomic ratio) shocked to an energy just below that for bulk reaction. Some thin interfacial mixed regions are observed as well as isolated pools of a mixture of Ni and Si. The more typical interfaces show no mixing.

## 5. SHOCK WAVE CONSOLIDATION OF A METALLIC GLASS

### 5.1 Shock Wave Consolidation of a Ni-Cr-Si-B Metallic Glass Powder

J. Bach, B. Krueger, and B. Fultz

W. M. Keck Laboratory of Engineering Materials

California Institute of Technology, Pasadena, California 91125

#### ABSTRACT

Bulk samples of metallic glass (Allied MBF 50) were obtained by shock consolidation of powder produced by ball-milling the as received ribbon. The amorphous samples exhibit low porosity and slightly higher hardness than the spun ribbon. Smaller distensions and longer shock durations favored good consolidation which was obtained with a powder distention of about 1.70 (particle size 44 to 88  $\mu\text{m}$ ) and shock energies between 140 and 200 J/g. Higher shock energies caused crystallization of the glass, and the shock front was shown to be planar and parallel to the flyer plate/sample interface.

#### INTRODUCTION

Since the pioneering work of Duwez,[1] many alloys have been discovered which solidify to an amorphous structure if cooled at a sufficiently high rate. To achieve the required cooling rate, typically greater than  $10^6$  K/s, at least one final dimension of the material must be small. Thus metallic glasses are usually available only in powder or ribbon form. In the present work we used shock waves to consolidate metallic glass powders into bulk compacts.

The deformation consolidation of metallic glass has been the subject of several previous studies. At moderate temperatures below the glass transition temperature, metallic glasses undergo a structural relaxation which, among other effects, causes an

increase in the viscosity of the material.[2] Since this relaxation is a time-dependent process, the instantaneous viscosity at a given temperature will be lower with higher heating rates.[3] On the other hand, the crystallization temperature of a metallic glass follows the opposite trend and increases with increased heating rate. In some metallic glasses, this decrease in viscosity and increase in crystallization temperature opens a time-temperature “window” in which it is possible to plastically deform and even consolidate the amorphous material without crystallization.[4] The fast thermo-mechanical cycle of the shock process would seem to offer a wide window for consolidation of many metallic glasses, and previous workers [5-9] have shown that the shock waves can successfully consolidate metallic glass powders.

It is doubtful, however, that the mechanism of consolidation is the same for shock consolidation, and for deformation consolidation at lower strain rates. The deformation of glassy metals changes from homogeneous to heterogeneous at the high stress levels of shock wave consolidation,[10,11] so shock wave consolidation probably does not depend on the time-temperature window provided by decreased viscosity and higher crystallization temperatures at high heating rates. An alternative possibility for the mechanism of shock consolidation is provided in the next section. In the present work we varied the shock parameters for the consolidation with the intent to find the range of shock pressures where consolidation was possible. We characterized these compacts to find the success of the consolidation and to learn how the deformation and bonding of the metallic glass particles occurred.

## SHOCK WAVES AND SHOCK CONSOLIDATION

The energy and pressure associated with the shock process are governed by the Rankine-Hugoniot relationship.[12] The details of shock wave physics will not be discussed, however one equation of interest is:

$$E = \frac{1}{2}P (V_0 - V_1) \quad (1)$$

where  $E$  is the deposited specific internal energy;  $P$  is the shock pressure;  $V_0$  is the specific volume of the initially porous material, and  $V_1$  is the shocked specific volume. For our work the shocked volume differs little from the solid specific volume of the material, so  $V_1$  can be replaced by the solid volume after consolidation. This results in the equation:

$$E = \frac{1}{2}P V_0 (m - 1) \quad (2)$$

which approximates the energy as being deposited in the form of thermal energy (where  $V_0$  is the solid volume at STP, and  $m$  is the distension,  $m=V(\text{powder})/V(\text{solid})$ ). The pressure in Equation 2 was determined according to the model proposed by Simons and Legner [13] for the compaction of porous materials. Although the model makes some simplifying assumptions, we believe it to be sufficiently accurate for the current work. Since the isentropic bulk modulus and Grüneisen parameter, the thermodynamic parameters required by their model, have not been determined for this alloy, we assumed these parameters were the same as for elemental nickel.

In a picture of shock consolidation provided previously by Kasiraj et al.,[14] densification and bonding of individual powder particles occurs within the shock front by pore collapse and the preferential deposition of energy near the particle surface causing local melting. They showed that in ductile materials the surface regions of the particles

are heated on a time scale of  $10^{-7}$  s. With such an energy deposition profile, the particle interiors remain at a relatively low temperature during the shock process, so if melt pools are formed at particle surfaces, they are solidified to an amorphous structure by heat flow into the particle interiors. The size of the melt pools must be below a critical value, depending on the properties of the material, in order for the consolidated material to be rapidly solidified into an amorphous structure. It is also important that the homogeneous temperature, the temperature to which the bulk material equilibrates, does not rise above the crystallization temperature, since heat conduction to the surroundings is relatively slow. This picture of shock consolidation is not based on the existence of the time-temperature window which permits the consolidation of metallic glasses at lower strain rates.

## EXPERIMENT

The material investigated was an amorphous alloy produced in ribbon form by Allied Corporation under the product name MBF50 with a composition of 76.4%Ni - 19%Cr - 2.3%Si - 1.5%B - 0.08%C (concentrations in wt.%). According to the manufacturer, its solid density and crystallization temperature are  $7.49 \text{ g/cm}^3$  and  $740^\circ \text{ K}$  respectively. The ribbon was ball milled into powder in an Argon atmosphere for about 8 h. The powder was sieved to obtain the desired particle size (the size for each shot is presented in Table I), loaded into a target, and compressed in a hydraulic press to the desired distention. A 35 mm smooth bore propellant gun [15] was used to propel either an AISI 303 stainless steel or a teflon flyer plate to impact the powder. The velocity of the flyer was measured using a radar doppler velocitometer and a time-of-flight optical interrupt system. The velocity was used to obtain the Hugoniot of the flyer [13] which was numerically compared to the Hugoniot of the powder in order to obtain the shock pressure. The pressure was then used in Equation 2 to calculate the energy.

The consolidated samples were polished and etched with Marble's reagent (4g CuSO<sub>4</sub>, 20cc HCl, 20cc H<sub>2</sub>O), and were examined with a Nikon Epiphot metallograph. For measurements of porosity, some micrographs were digitized and mapped into a binary form with a television system interfaced to a Macintosh II computer that ran a public domain image analysis software program, Image. Density measurements were also performed by the Archimedes method, but these measurements were accurate to only 1-2%. To measure crystallization temperatures, differential scanning calorimetry (DSC) was performed with a Perkin Elmer DSC-4 operated at various heating rates. X-ray diffractometry was performed with a Norelco  $\theta$ -2 $\theta$  diffractometer with Cu K $\alpha$  radiation and digital data acquisition.

## RESULTS AND DISCUSSION

A total of eight shots were executed, with shock energies ranging from 133.8 J/g to 364.6 J/g as listed in Table I. Three of the shots resulted in amorphous compacts, three resulted in partial or total crystallization of the samples, and two shots, with the lowest shock energy, resulted in only partial bonding of the particles.

Figure 1 shows the consolidated compacts, one of which was prepared for compression tests. Macroscopic cracking occurred in some of the consolidated samples, but the piece of material at the center of Figure 1 was apparently free of cracks. Optical microscopy revealed that the compaction process caused heavy plastic deformation in the initially spherical particles (Figure 2). This implies large localized strains, which suggest large local heterogeneities in the deposition of the shock energy.

Our metallographic porosity measurements showed porosity between 0.64% to 1.77%, with the lower densities corresponding to the lower shock energies (an example is presented in Figure 3). Density measurements by the Archimedes method confirmed this trend.

The amorphous states of the ribbon, ball milled powder, and the compacts were verified using x-ray diffractometry (Figure 4). The crystallographic states of the compacts obtained with various shock parameters are presented in Table I. For shock energies below 140 J/g, the consolidation of the powder was incomplete, although it remained amorphous. For shock energies above 200 J/g the compact was at least partially crystalline. Comparison of the broad diffraction peaks of the amorphous and partially crystalline compacts showed that for shock energies above 200 J/g crystallization occurs gradually rather than abruptly, indicating a locally heterogeneous thermomechanical history. For compacts that were fully amorphous, we scrutinized the widths and positions of the broad diffraction peaks at  $2\theta = 45^\circ$ , and it appeared that the average first neighbor distance in the compact was slightly ( $< 1\%$ ) larger than that of the melt-spun ribbon. The DSC heating curves of the ribbon, ball milled powder, and compacts had nearly the same integrated areas, although the crystallization exotherms for the powder and compacts were somewhat broader than for the ribbon.

The DSC runs were performed at different heating rates, and showed that the onset of crystallization increases by about 30 K per decade of heating rate. Extrapolation of the crystallization temperature vs. heating rate curve results in an increase in the onset of crystallization from  $471^\circ\text{C}$  (at  $dT/dt = 20^\circ$  per minute) to  $582^\circ\text{C}$  (at  $dT/dt = 10^6$  degrees per minute).

One of the samples, obtained with a 303 stainless steel flyer impacting at a velocity of 1060 m/s, was found to be crystalline at the impact side to a depth of about 3 mm, and amorphous at the opposite side. The interface between the layers, seen in Figure 2, was sharp and its parallel orientation shows that the shock wave is planar. The high energy of the shock wave caused crystallization of the first half of the sample. However, the pressure of the primary wave was reduced upon the arrival of the release wave (the unloading reflection from the junction between the flyer plate and the

supporting sabot), and the rest of the sample was consolidated while preserving its amorphous state.

The Vickers miniload hardness data were slightly higher for the amorphous compacts ( $HV=800+Kp/mm^2$ ) than for the ribbon ( $HV=650Kp/mm^2$ ). Two very different hardness values were obtained for the crystalline samples. X-ray diffractometry showed that these different hardness values corresponded to different crystal structures, and we believe that differences in the crystalline phases are at least partially responsible for the different hardness of the crystalline compacts. DSC showed a strong exotherm at a hundred degrees above the crystallization temperature, which was shown by x-ray diffractometry to correspond to the same change in the crystalline phases.

Taking the total shock energy to be deposited as heat, the low shock energies of 140 J/g correspond to a homogeneous temperature of 335° C, and the highest shock energies of 200 J/g for which the compact remained amorphous corresponded to a homogeneous temperature of 470° C (which is the crystallization temperature). The Markomet 1064 consolidated previously by Kasiraj, et al.[6] remained amorphous to higher shock energies (~400 J/g), but the crystallization temperature of the Markomet 1064 was 700° C. Kasiraj et al.[6] noted that 400 J/g corresponded to a homogeneous temperature that was higher than the crystallization temperature of their Markomet 1064, but no such effect was observed in the present study. Finally, we believe it is coincidental that this temperature range for consolidation by heterogeneous deformation seems consistent with the temperature window for consolidation by homogeneous deformation extrapolated to very high heating rates. From measurements of the shock risetime of  $10^{-7}$  s [14,16], the shock front is on the order of one particle diameter (60  $\mu$ m). Energy deposition occurs within the shock front, and using typical thermal conductivities of Ni alloys, during the shock risetime the characteristic distance for thermal conduction is about 1- $\mu$ m. High temperatures and melting could readily occur at the surfaces of the particles, assuming that the surface regions are preferential sites for

heterogeneous deformation. It is probably necessary that some of the deformation occurs in the particle interior, however, since a 1  $\mu\text{m}$  surface layer is too small to absorb all of the shock energy without vaporizing.

## CONCLUSIONS

We obtained bulk samples of metallic glass by shock wave consolidation of ball-milled powder. The amorphous samples exhibit low porosity and slightly higher hardness than the commercially spun ribbon. Smaller distentions and longer shock durations produced better compacts. The energy range for a successful consolidation is 140-200 J/g for powder of particle size  $44 < d < 88 \mu\text{m}$  and distention of about 1.70. Our observations are consistent with a mechanism for shock consolidation that relies on a high energy deposition near the surfaces of the particles, and probable melting of the particle surfaces. The shock front was shown to be planar and parallel to the flyer plate/sample interface.

## ACKNOWLEDGEMENTS

Helpful conversations with Andy Mutz, and differential scanning calorimetry work by Zezhong Fu and Lawrence Anthony are gratefully acknowledged. Barry Krueger died on October 29, 1990 from injuries received in a motorcycle accident. We thank Allied Chemical for the donation of the material. One of the Authors, J. Bach, acknowledges the support of the Summer Undergraduate Research Fellowship program at the California Institute of Technology. This work was supported in part by the National Science Foundation grant DMR – 8811795.

## REFERENCES

- [1] P. Duwez, *Fiz.-2 Suppl.* 2, 1 (1970).
- [2] A. I. Taub and F. Spaepen, *Scripta Metall.* 13, 195 (1979).
- [3] A. I. Taub, *Acta Metall.* 30, 2117 (1982).
- [4] P. H. Shingu, *Mater. Sci. Eng.* 97, 137 (1988).
- [5] C. F. Cline and R. W. Hopper, *Scripta Metall.* 11, 1137 (1977).
- [6] P. Kasiraj, D. Kostka, T. Vreeland, Jr., and T. J. Ahrens, *J. Non-Cryst. Solids* 61, 967 (1984).
- [7] D. Raybould, D. G. Morris, and G. A. Cooper, *J. Mater. Sci.* 14, 2523 (1979).
- [8] D. G. Morris, *Metal Sci.* 14, 215 (1980).
- [9] L. E. Murr, S. Shankar, A. W. Hare, and K. P. Staudhammer, *Scripta Metall.* 17, 1353.(1983).
- [10] F. Spaepen and A. I. Taub, "Amorphous Alloys: Flow and Fracture," General Electric Report No. 83CRD068 (April 1983).
- [11] F. Spaepen, *Acta Metall.* 25, 407 (1977).
- [12] Y. B. Zel'dovich and Y. P. Raizer in "Physics of Shock Waves and High Temperature Hydrodynamic Phenomena, Vol. 2," W. D. Hayes and R. F. Probstein (eds.), Academic Press, New York, 685-715 (1966).
- [13] G. A. Simons and H. H. Legner, *J. Appl. Phys.* 53, 943 (1982).
- [14] R. B. Schwarz, P. Kasiraj, and T. Vreeland, Jr. in "Metallurgical Applications of Shock-Wave and High-Strain-Rate Phenomena," L. E. Murr, K. P. Staudhammer, and M. A. Meyers (eds), Marcel Dekker, New York, 331 (1986).
- [15] J. Bach, "Shock Wave Consolidation of Metallic Glasses," Proceedings Fourth National Conference on Undergraduate Research, Vol. 1, Univ. N. Carolina, Asheville, 194 (1990).
- [16] R. B. Schwarz, P. Kasiraj, T. Vreeland, Jr, and T. J. Ahrens, *Bull. Am. Phys. Soc.* 28, 460 (1983).

SHOCK ENERGY (J/g)	POWDER SIZE $\mu\text{m} < d < \mu\text{m}$	DISTENSION	FLYER Material/ Thick.(mm)	VICKERS	COMMENTS
364.6	$d < 88$	1.84	303SS/5	853 171	AMORPHOUS REGION CRYSTALLINE REGION
285.2	$44 < d < 88$	1.84	303SS/9.28	906	MOSTLY CRYSTALLIZED
209.7	$44 < d < 88$	1.72	303SS/9.02	731	AMORPHOUS
197.1	$44 < d < 88$	1.73	Teflon/9.98	990	PARTIALLY CRYSTALLIZED
163.1	$44 < d < 88$	1.73	303SS/9.23	800	AMORPHOUS
141.4	$44 < d < 88$	1.74	Teflon/9.96	815	AMORPHOUS
134.9	$d < 44$	1.70	303SS/8.97	715	PARTIALLY CONSOLIDATED
133.8	$44 < d < 88$	1.70	303SS/9.02	625	PARTIALLY CONSOLIDATED

Table I. Shock conditions for the various shots. The first row shows the conditions for the shot in which the compact obtained was crystalline on the impact side and amorphous on the target side. Vickers hardness for the amorphous MBF/50 ribbon is 653.

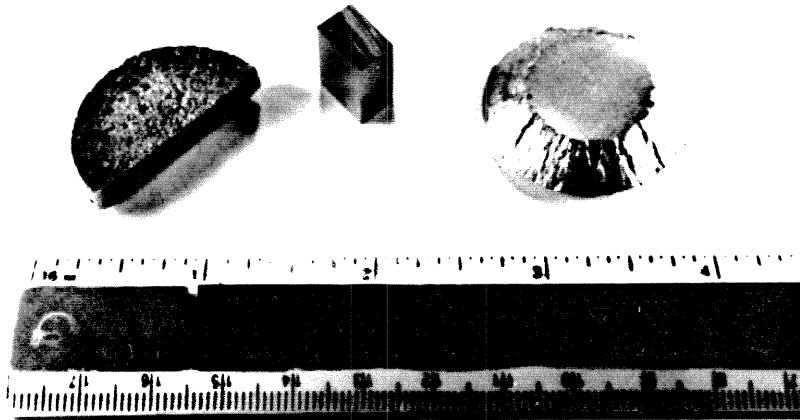


Figure 1. Photograph of recovered compacts. On the left is the sample which crystallized to a depth of about 3mm, on the right is amorphous sample, and in the center is amorphous sample prepared for compression testing.



Figure 2a. Optical micrograph of the compact shown on the left in Figure 1 showing the transition region. The shock wave propagated from left to right.



Figure 2b. A macro-photograph of the polished and etched compact. The shock wave propagated from left to right.

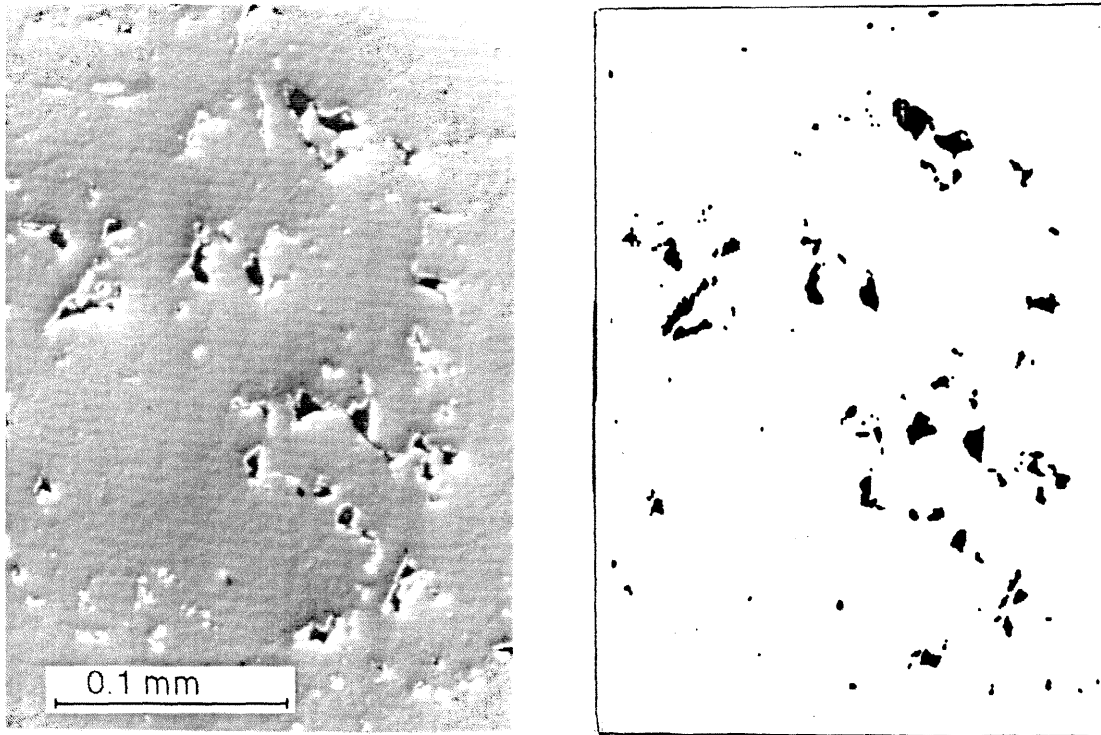


Figure 3. A typical micrograph and binary map used to calculate porosity.

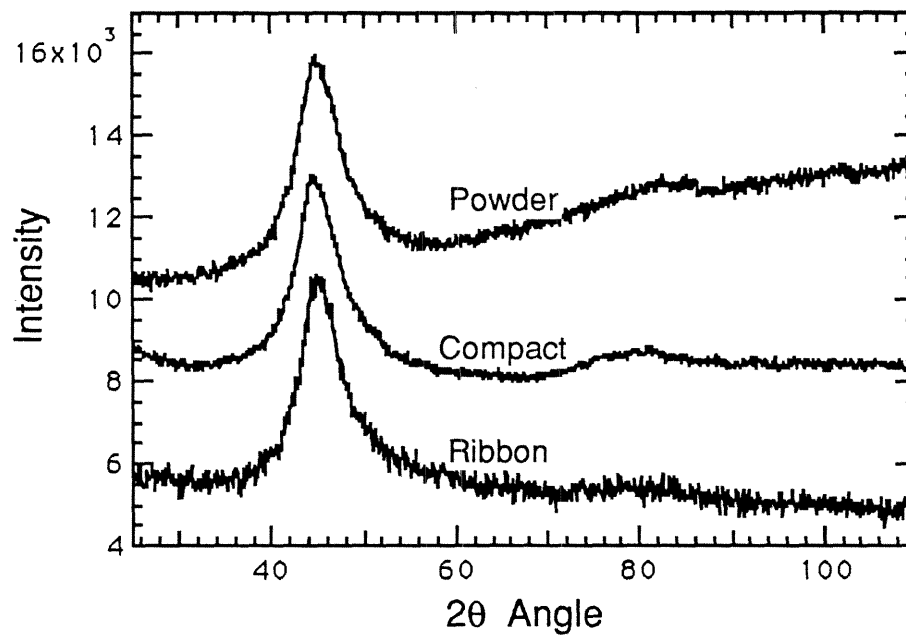


Figure 4. Cu K $\alpha$  diffractometer scans of Allied MBF/50 ribbon, ball milled powder, and compact obtained with shock energy of 163.1 J/g.